LAWRENCE
LIVERMORE
NATIONAL
LABORATORY

LLNL-JRNL-609897

Boron: a frustrated element

T. Ogitsu, E. Schwegler, G. Galli

January 11, 2013

Chemical Reviews

Disclaimer

Boron: a frustrated element

Tadashi Ogitsu, Eric Schwegler, and Giulia Galli

Abstract

In the periodic table boron occupies a peculiar, crossover position: on the first row, it is surrounded by metal forming elements on the left and by non-metals on the right. In addition, it is the only non-metal of the third column. Therefore it is perhaps not surprising that the crystallographic structure and topology of its stable allotrope at room temperature (β-boron) are not shared by any other element, and are extremely complex. The formidable intricacy of β-boron, with interconnecting icosahedra, partially occupied sites, and an unusually large number of atoms per unit cell (more than 300) has been known for more than 40 years. Nevertheless boron remains the only element purified in significant quantities whose ground state geometry has not been completely determined by experiments. However theoretical progress reported in the last decade has shed light on numerous properties of elemental boron, leading to a thorough characterization of its structure at ambient conditions, as well as of its electronic and thermodynamic properties. This review discusses in detail the properties of β-boron, as inferred from experiments and the ab-initio theories developed in the last decade.

I. Introduction

At the beginning of the 21st century, the properties of most of the elements—at least the ones with stable forms that can be isolated at ambient conditions—are well understood. The fundamental properties of elements, including the thermodynamic stability of their allotropes and polymorphs, have been compiled and published in many books.[1] Only the fifth element of the periodic table, boron, has eluded a complete characterization, and its thermodynamic stability at ambient pressure has not yet been established by experiments (see Figure 1).[2] Boron displays a large family of allotropes, 16 in total, which is second in size only to sulfur.[1a] In spite of the important progress of the last few years in understanding the phase diagram of boron, there are still conflicting views in the literature, e.g. concerning the stability of two of its allotropes at low pressure, β- and α-rhombohedral,[3] and on the existence of the allotrope T-50. [4]

At ambient pressure, liquid boron solidifies into the β-rhombohedral phase, [5] indicating that this phase is the thermodynamically stable one at high temperature (T). β-boron has an extremely complex structure, with more than 300 atoms per unit cell, that consists of a combination of icosahedra and fused icosahedra; a phase transition from β-boron to other phases—by cooling or annealing at ambient pressure—has never been reported. In fact, early reports suggested that β-boron is likely to be the thermodynamically stable phase of boron for all temperatures below melting at ambient pressure,[6] down to at least ~1400 K.[3b,7] However these reports lacked a quantitative comparison of the thermodynamic stability of different phases, due to the lack of robust measurements of formation enthalpies. The high melting temperature and chemical inertness of β-boron makes it challenging to accurately estimate its enthalpy of formation from calorimetric measurements.

Nevertheless, β-boron would have been accepted as the de facto stable phase at all temperatures at ambient pressure if the so called electronic requirement—a closed shell–electronic structure—and the thermodynamic requirement—a perfect crystal structure—were clearly satisfied; but these requirements are apparently violated [8] in β-boron. For example, experiments have revealed that β-rhombohedral boron possesses a macroscopic amount of intrinsic defects[8c] for which no ordering has been observed. In addition, although an electron count does not reveal a closed shell structure, the transport properties of the system appear to be similar to those of a nearly closed shell–electronic structure solid. In particular β-boron "behaves" like a p-type semiconductor,[9] with a very low electronic conductivity [8c] and an optical gap of about 1.5 electron volts (eV). [8c,10]

Theoretical and computational approaches have played a crucial role in understanding boron and its compounds. Early molecular orbital (MO) calculations elucidated two key concepts in the chemistry of boron. First, the peculiar molecular structure of diborane has been shown to arise from the formation of three-center, two-electron (3c2e) bonds.[11] Second, MO theory predicted the charge state of $B_{12}H_{12}^{-2}$,[4b] which was later confirmed by the successful synthesis of di-potasium salt, $K^{+}_{2}B_{12}H_{12}^{-2}$.[12] As we shall show, those two concepts—3c2e bonds and the presence of slightly electron deficient (2e) boron icosahedra in elemental boron—are key to understand the nature of boron allotropy.

The second wave of theoretical developments came about with density functional theory (DFT) and high-performance computers, which made it possible to perform most of the calculations on the bulk structures of boron available to date. The first theoretical study of the electronic structure of β-rhombohedral boron[8b] did not include intrinsic defects and resulted in an

incomplete occupation of the valence band, and its author concluded: “Hence, a deformed structure occurs in which some atoms are randomly displaced into interstitial sites.” [8b] This suggested that intrinsic defects play a role in determining the electronic structure of boron and in satisfying electronic requirements.

The mechanism of self-doping caused by the intrinsic defects was not fully understood until 2007–2009,[3f,3i,3k] although it had been discussed in earlier studies.[3d,13] It is now understood that the interplay between the imbalance of electron requirements between the B_{12} [4b,12] and B_{28} [3d,3k,13b,14] units present in β-rhomohedral boron, the local intrinsic instability of B_{28},[3k,14] and the conversion of two-center, two-electron (2c2e) bonds to 3c2e bonds due to the presence of self-interstitials, all lead to a nearly perfect closed shell–electronic structure.[3k] The defects are necessary to stabilize β-boron; this means that in β-boron defects have a negative formation energy.[3e,f,3i,3k,13a,14a,15] Within first principles–DFT calculations, β-boron is found to be the most energetically favorable allotrope of boron at ambient pressure and at all temperatures below melting, when a macroscopic amount of defects is present.[3f,3i,3k]

Many defect configurations—including various combinations of vacancies and self-interstitials—exhibit exactly the same energy, leading to a disordered and degenerate ground state for β-boron, with a macroscopic amount of residual entropy. The mechanism that leads to the multiplicity of geometrical configurations is called geometrical frustration,[3l] a property exhibited also by ice and magnetic–spin ice materials.[16]

Proton disorder in ice and spin disorder in magnetic pyrochlore materials may be described with the same type of Hamiltonian used to describe defects in boron, that of a ferromagnetic Ising model on corner–sharing tetrahedral.[16g] Within a nearest neighbor–

interaction approximation, this Hamiltonian has an exactly degenerate and disordered ground state with a macroscopic amount of residual entropy.[16g]

The calculated specific heat of spin ice as a function of temperature, obtained by using a ferromagnetic Ising model with nearest neighbor (NN) interactions, shows excellent agreement with experiments, thus supporting the existence of a degenerate ground state with macroscopic entropy.[16h] However the use of a more accurate spin-spin interaction-- dipole-dipole interaction-- and of an advanced cluster–update algorithm, shows that the dipole Ising model exhibits a phase transition to an ordered phase at very low temperature (below 0.2 K).[16h] The spin-spin correlation measured by neutron scattering, is in better agreement with a dipole Ising model than with an NN Ising model, suggesting that the dipole Ising model is a better approximation of spin ices: however a phase transition to an ordered phase has never been never observed in real materials.[16h] Therefore, it was tentatively concluded that the observed residual entropy of spin-ices is a non-equilibrium property due to the slow dynamics at low temperature, and that such systems are likely to have a nearly degenerate ground state, not an exactly degenerate one.[16h]

In this review, the description of boron ground-state properties parallel the interpretation of the residual entropy adopted in the case of spin ices: An exact degeneracy is unlikely to exist in elemental boron, if cooled down to a T very close to zero. At finite T, the system is nearly degenerate. The identification of a model Ising Hamiltonian that describes the defects' configurations was instrumental to understand how the macroscopic (near) degeneracy can be realized[16c,16g,17] at finite T.

As the case of spin ice shows, the comparison of the specific-heat profile obtained from theoretical models and experimental measurements plays an important role in understanding how geometrical frustration leads to a nearly degenerate ground state with macroscopic residual

entropy.[16g] In the case of boron, unfortunately, no attempt has been made to measure the impact on the specific heat of different defect configurations. Therefore, the near degeneracy in the configuration of defects has not yet been confirmed experimentally. Many experimental studies reported evidence of defect diffusion in β-boron, which was considered as one of the leading causes of the anomalies in the transport properties[9-10,18] and in internal friction data.[18a,18j,k] It was also shown that the optical absorption of β-boron exhibits a dramatic change as a function of temperature at about 150–200 K.[18l,m] Below this temperature range, only a few absorption peaks appear in the optical gap, but their number greatly increases above ~ 200 K. A structural phase transition was suspected to occur at this T, but it was not evident from X-ray diffraction measurements.[18a]

Given that many of the anomalies in the transport properties are observed at 150-200 K, it was first suggested that they are probably due to the diffusion of defects.[18a,18l,18n] Later observations, however, seem inconsistent with the notion of defect diffusion in boron. For example, the occupation rates of the partially occupied sites (POS) show clearly measurable differences depending on the synthesis conditions, and the difference in the occupation rates persisted for more than several years after annealing at ambient conditions.[8c] If boron interstitials diffused below a temperature of 150 K,[18n] they should, it seems, reach an equilibrium occupation configuration within a reasonable time scale: if so, the occupation rates would be the same in different samples, after a sufficiently long annealing time. Apparently, this is not the case.

To resolve this issue, the activation barriers between many different occupation configurations—whose total energies are nearly degenerate—were determined by first principles–DFT calculations.[3l] This revealed a few boron-hopping paths with low enough activation energies to allow for defect diffusion at low temperature. However, some of the

activation energies were found to be of the order of several eV, thus unlikely to allow for atomic diffusion. Their presence might explain the persistent difference in the occupation rates of POS in samples obtained by different annealing procedures. The lowest-energy activation mechanism involves only defect locations belonging to the same crystallographic site; therefore, in this case defect diffusion does not change the occupation rate.[31] Among the configurations visited during diffusion, there are geometrical arrangements responsible for introducing significant gap levels in the electronic band structure of β-boron.[31]

Several recent articles have reviewed the properties of boron, including the chemistry of borane and boride,[19] the phase diagram of elemental boron under pressure,[20] the chemistry of boron clusters,[21] experimental measurements on β-boron,[22] and the electronic and mechanical properties of boron and boron-rich compounds.[23] This review focuses on the recent theoretical advances in describing the properties of β-rhombohedral boron. The other allotropes, α-rhombohedral, T-50 (or T-192), and γ-B_{28}, were reviewed by Albert and Hillebrecht in 2009,[19b] therefore, in this article, only new developments since 2009 will be briefly discussed (α-boron,[23-24] γ-B_{28},[25] T-50[4l-n]).

We will first describe the crystal structure of β-rhombohedral boron and the partial occupancy of defect sites (that we call, following the literature, partially occupied sites or POS). We will then discuss β-boron's thermodynamic stability, which in recent years has been extensively investigated by theorists, and geometrical frustration. We will then present an analysis of the electronic properties. We conclude with few comments on the third law of thermodynamics and on prospects of future boron research.

II. β-rhombohedral boron: From its identification to the establishment of partial occupancy

In this section, we review how the crystal structure of β-rhombohedral boron and its partial occupancy were established. We also briefly discuss the discoveries of other major allotropes: α-rhombohedral,[26] α–tetragonal (or T-50),[4c-g,4j,k] β-tetragonal (T-192),[4g,27] and γ-B_{28}.[2,28]

Elemental boron was successfully isolated in 1900–1910[29] and diffraction patterns were first taken in the 1930s.[30] Methods for synthesizing boron were established from 1940 through the 1950s,[3a,4a,4c,5a,26,31] which revealed the presence of various polymorphs and allotropes. Most of these allotropes have complicated crystal structures based on icosahedra, which were only identified in the 1950s.[3a,4a,26a] Except for the simplest forms—α-rhombohedral boron[26a] and, perhaps, γ-B_{28}, which was discovered in 2009[2,28b]—uncertainties remain about the structure and physical properties of boron's allotropes.

The first crystal of α-tetragonal boron was identified in 1951,[4a] and it was called T-50, from the 50 atoms in its tetragonal unit cell. In 1955, based on the electron requirements of the $B_{12}H_{12}$ cluster estimated from MO theory, it was reported that the T-50 structure is 10 electrons short of filling all bonding orbitals (or valence bands).[11a] This suggested that a pure form of T-50 would not be stable.[4b] In 1958, additional experiments[4c] seemed to confirm the existence of T-50, but from the late 1960s to the mid-1970s it was demonstrated that only $B_{48}B_2C_2$ or $B_{48}B_2N_2$ compounds were in fact synthesized.[4d-f,32] It was later reported that the pure form of tetragonal boron has a structure similar to α-AlB_{12} with partial occupancy, and it was described as $B_{21}2B_{12}B_{2.5}$.[4g,27b] This structure is a combination of entwined icosahedra, regular icosahedra, and

interstitials; this phase, first reported in 1960,[4g,27a,b] was named T-192. The controversy around the T-50 phase continued for many years, and theoretical studies eventually supported the notion that T-50 can only be stabilized in the presence of impurities.[4j,k] Very recently, three independent groups[4l-n] have reported on the identification of this phase as pure elemental boron, and have suggested that T-50 appears as a meta-stable phase due to the Ostwald step rule.[33]

In 1957, Sands and Hoard announced the identification of the β-rhombohedral phase, which belongs to the space group $R\bar{3}m$ with a lattice parameter (a) of 10.12Å, a rhombohedral angle (α) of 65°28′, and an approximate atomic density of 108 atoms per rhombohedral cell.[3a] In 1960, Hoard and Newkirk reported that many of the synthesized pure-boron solids from studies completed in 1930–1950 were likely to contain the β-rhombohedral phase.[3b] In the early 1960s, the thermodynamic stability of β-rhombohedral boron at high temperature was established,[5] and some reports suggested that it is thermodynamically stable at all temperatures, but these conclusions were based on indirect evidence.[3a,b] To date, no experiment has unequivocally determined the thermodynamic stability of this phase.

In 1962, X-ray analysis provided a partially correct report of the atomic positions of β-rhombohedral boron.[34] In 1963, the main crystallographic features of the system were reported: the structure was described as being composed of 12 half icosahedra surrounding a larger icosahedron (84 atoms) and 20 more atoms connecting these B_{84} units in adjacent unit cells (see Figure 2).[6] In 1970, an additional crystallographic position, B16, was identified by Hoard *et al.* [8a] This work also reported partial occupancy at B13 and B16 sites, but with a slight inconsistency in the atomic densities estimated from fitting X-ray derived positions, and from floatation-measurements.[8a] Two other independent studies from about the same period, by Geist *et al*. [35] and Callmer,[36] refined the atomic positions in β-boron; the former did not report the presence of

partial occupancy but the latter did. However the lattice parameters and the atomic positions from these three papers from the 1970s are in excellent agreement with each other. Donohue[1a] suggested that the partial occupancy reported by Hoard *et al.* "may possibly [be] due to the somewhat lower purity of the sample used…." He adds: "It is also difficult to understand why the standard errors of Hoard *et al.* are only one-third, on the average, those of Geist *et al.* The fewer number of reflections used by the latter by no means can account for this discrepancy."

In 1988, Slack *et al.* [8c] reported the presence of four more POS based on a study that carefully investigated the correlation between the impurities and the synthesis conditions and their influence on the occupation rates of POS, and on the atomic density; such investigation turned out to be crucial for later theoretical studies. This research team also suggested a few possible short-range correlations between the occupation configurations of POS. In addition Slack *et al.* reported the electric conductivity of β-boron; the impurity-free limit extrapolated from several measurements confirmed the semiconducting properties of the system (resistivity of the order of 10^{-8} Ω cm). It is fair to say that the work of Slack established the presence of partial occupancy in elemental boron.

The α-rhombohedral phase of boron was identified shortly after the discovery of the β-rhombohedral one. [26] This structure consists of a single icosahedron in a slightly distorted cubic cell,[26b] with the C3 axis of the icosahedron aligned to the c-axis of the unit-cell. This geometrical arrangement indicates that the formation of three 3c2e external bonds (called delta bonds at the time) and of 2c2e external bonds may yield a closed shell–electronic structure, which was later confirmed.[37] In the past decade, several theoretical studies[3c-e,3h,13b,15] have addressed the relative thermodynamic stability of the α– and β-rhombohedral phases. Contrary to the earlier suggestions by experimentalists, some theoretical calculations reported that α-boron should be

the stable phase at low temperature and ambient pressure, but these results were obtained with an approximation that takes into account only the partial occupancy of B13 and B16[3c-e,13b,15] sites. Later, three independent theoretical studies showed that incorporating the POS originally omitted makes β-rhombohedral more stable than α-rhombohedral boron.[3f,3i,3k]

A new high-pressure phase of boron, γ-boron, discovered in 2009, consists of icosahedra and interstitials, [2,28b] and it exhibits an ionic character.[2,25l] This property originates from the electron deficiency of the icosahedra,[4b,12] which seems to prove the universal ionic character of icosahedra-based phases of elemental boron.[2,4b,12-13,14a,25l,38] An iso-structural phase transition of γ-boron was proposed by Zarenchnaya *et al.* in 2010,[25b] however, later theoretical and experimental studies consistently rejected this view. [25n,25p]

At the time of writing this review, the crystal structure of the superconducting high-pressure phase discovered in 2001[39] has not yet been identified; theory suggests it may be the α-Ga (Cmca) structure.[40] Although some studies[41] suggest different scenarios, enthalpy comparisons indicate that the α-Ga structure is indeed the most likely candidate for the structure of the superconducting phase.[2,40a] Interestingly, different approaches based on compression of α-boron[24b] and Li doping of α-boron,[24d,e,42] originally proposed by Gunji *et al.* in 1993,[42a] have also successfully observed a phase transition to a superconducting phase.[24a,b,24d,42h] We note that the superconducting phase obtained by compression of α-boron retains its original crystal symmetry most likely as a meta-stable state, with metallization achieved by band overlap.[24b,42h]

Before turning to the discussion of the detailed structure of β-rhombohedral boron, it is interesting to draw a comparison between the boron crystal structures and those of the other group III elements. In 2003, Haussermann *et al.* [40a] calculated the phase diagram of group III elements—boron, aluminum, and gallium—and compared the α-rhombohedral (bct and fcc) and

α-Ga crystal structures. Interestingly, in the case of boron, they found that the α-Ga structure, rather than bct or fcc, is the most stable phase above 74GPa. They also identified the stable pressure ranges for the α-rhombohedral phase of aluminum and gallium. In 2004, Ma *et al.* [40b] studied the superconductivity of the α-Ga phase of boron, and they reported that the pressure dependence of the electron-phonon coupling constant is consistent with experimental observations. Consequently, they suggested that the α-Ga phase might be a good candidate for the high-pressure metallic phase of boron.

Extensive work on the Zintl phase–p block intermetallic compounds—group III elements—showed that they form icosahedral clusters. Therefore, one might think that the ability to form such clusters is a general property of trivalent elements with 2s and 1p valence electrons, which raises the question: Why does only elemental boron form icosahedra-based crystal structures? The α-rhombohedral phases for aluminum and gallium appear in the negative pressure range.[40a] It is perhaps the localization length scale of the valence orbital that singles out boron from the rest of group III elements.

III. The crystal structure of β–rhombohedral boron

In 1974, Donohue[1a] described the crystal structure of β-rhombohedral boron by writing: "The structure consists of an enormously complicated framework of boron atoms which contains, however, some simple and beautiful features which would have made Kepler leap with joy." This refers to Kepler's 16th-century study of packing two-dimensional space with pentagons.[43]

The crystal structure of β-rhombohedral boron was first described based on one B_{84} unit, $2B_{10}$ cluster units, and one interstitial.[6,8a] The B_{84} unit comprises a central icosahedron

surrounded by 12 half icosahedra (see Figure 2-a). The outer shell of B_{84} consists of 60 boron atoms creating the same structure as that of a C_{60} fullerene molecule.[44] B_{84} units in adjacent unit cells are connected via B_{10} cluster units (see Figure 2-b). The interstitial atom (in Figure 2) is located between two B_{10} clusters. In this review, we use an alternative explanation of the crystal structure based on B_{12} icosahedra and B_{28} triply fused icosahedra, which makes it easier to rationalize the relationship between the atomic and electronic structure.

The rhombohedral cell of β-boron consists of an outer layer of 20 icosahedra—8 at the corners and 12 along the edges of the cell—and two triply fused icosahedra in the middle, which are connected by an interstitial boron atom (see Figure 3-a and -b). The cluster units may be connected by conventional 2c2e bonds (see Figure 3-c). Many reports have summarized the lattice parameters of β-boron,[3k] and they are all in a good agreement. For example, one well accepted report[6] provides the following parameters: a=10.145±0.015Å and α=65°17′±8′. This rhombohedral angle—slightly larger than the one for a cubic lattice, which is 60°—allows this system to accommodate the B_{10} clusters, which are part of the B_{28} triply fused icosahedra (see Figure 2-b and 3-b). As we will discuss later, B_{28} plays an important role in counter balancing the electron deficiency of B_{12}.

Five crystallographic POS are compatible with rhombohedral symmetry (space group $R\bar{3}m$) and are described in the following. (This review uses the standard naming scheme for the crystallographic sites. [8c])

B13 is a vacancy site in the B_{28} triply fused icosahedra unit (see Figure 4). There is a simple reason for the presence of B13 vacancies: The total number of electrons in B_{28} (3×28) is too large for a closed shell–electronic structure when all of the external bonds are formed. The vacancy formation in triply fused icosahedra was first rationalized in the case of α–Ga_{28} clusters,

which appear in Zintl-phase intermetallic compounds.[14a,45] All recent first-principles studies on bulk β-rhombohedral boron confirm that full occupancy of the B13 site is not energetically favored.[3c-k,13b,15]

The structure of β-boron includes several additional POS whose occupation rates have been reported, e.g. in Ref. 8c (See Table 1). A B16 self-interstitial exists in the middle of the hexagonal ring connecting the B_{12} icosahedra (see Figure 5). B19 and B20 interstitials lie in the hexagonal rings connecting B_{12} and B_{28}, (see Figure 6 and 7). B17 and B18 interstitials are next to each other and surround the B13 vacancy sites (see Figure 8). We will see that these locations—B16, B19, and B20 being at the center of hexagonal rings, and B17 and B18 surrounding B13 vacancy sites—are key to understanding the effect of POS on the stabilization and electronic structure of β-boron. Ultimately, the knowledge of POS locations provides a coherent picture of the observed number of partially occupied sites and of the atomic density of 320 atoms per hexagonal cell; it also helps explain the observed electronic properties—that of a p-type semiconductor with a very low electronic conductivity—without requiring any long range ordering of the arrangement of partially occupied sites. Finally, it explains why the observed fluctuation in the occupation rates does not affect the electronic properties, as we will discuss in detail in Section *VI*.

Another important aspect of the POS layout in β-boron is its connection to a two-dimensional kagome lattice. In fact, the POS form a double layer–expanded kagome lattice (see Figure 9–11). This lattice plays an important role in determining the thermodynamic properties of boron, and in explaining the observed anomalies in the temperature dependence of the transport properties. In 1958, Frank and Kasper noticed the close relation between rhombohedral symmetry and a kagome network. [46] In 1977, Hughes *et al.* reported that the icosahedra in β-

boron at z=c/2 (where c is the length of the rhombohedral unit-cell along the z-axis) form a kagome network, and added: "Finally, and dramatically, the B_{28}-(C3v) unit … occupies the same tetrahedral hole in the β-B105-($R\bar{3}m$) structure, preserves one of the threefold axes of $Fd\bar{3}m$, and produces the observed rhombohedral symmetry" [47] (See Figure 12). However it is only in 2010 that the impact of a kagome network in the crystal structure on boron thermodynamic properties, was pointed out. [31]

IV. Thermodynamic stability of β-rhombohedral boron

In this section, we review the studies—first experimental and then theoretical—of the thermodynamic stability of β-rhombohedral boron. As already noted, liquid boron has been observed to solidify only into the β-rhombohedral boron phase.[5] Moreover, when heated at about 1773K, α-rhombohedral boron transforms to the β-rhombohedral phase.[26b] Several experimental studies[6,7b] indicated that the α-to-β phase transition is irreversible, and Carlsson [7b] pointed out that "a large increase in the time required for the transformation with decreasing temperature was observed indicating a large activation energy. This means that a practical limit for observing the transformation may be about 1000 C." This indicates that, within the temperature range studied in Ref. 7b, the free energy of β-rhombohedral boron is lower than that of α-rhombohedral boron, but slow kinetics precluded the determination of the range of stability of α-rhombohedral boron at lower temperature. Machaldze observed the α-to-β phase transition over the range 1723~1985 K, at ambient pressure.[48] The measured heat of transformation, *dH*=-1.05 kcal/mol, indicates that the transformation is exothermic. In 2011, Parakhonskiy *et al.* performed high-pressure and high temperature experiments and identified a α–β coexistence line at high pressure. Based on a linear extrapolation, they proposed that the α–β phase boundary at P=0 GPa is at T=933(50) K.

In 1992, Mailhiot *et al.* [49] reported the first extensive study of boron phase boundaries based on first principles–DFT calculations. They computed enthalpy curves of various conceivable polymorphs of boron and of the α-rhombohedral phase up to two-fold volume compression. They considered several polymorphs: body-centered-tetragonal (bct), diamond structure, simple cubic (sc), face-centered cubic (fcc), and hexagonal closed pack (hcp). At low pressure, the α-rhombohedral phase was found to be the most stable. It transforms to bct at 210 gigapascals (GPa) and to fcc at 360 GPa. Inspired by theoretical predictions on the high T_c superconductivity of the lightest elements[50] and by the high-pressure phase diagram predicted by Mailhiot *et al.,*[49] Eremets *et al.*[39] compressed β-rhombohedral boron close to 260 GPa and found that it exhibits superconducting properties above 160 GPa. The crystal structure of the superconducting phase, however, has not yet been experimentally identified. Based on the predicted crystal structures, bct or fcc, Papaconstantpoulos and Mehl[41a] and Bose *et al.* [41b] calculated the superconducting transition temperature as a function of pressure, which showed the opposite trend as compared to the experiments.[39]

The stability of boron at low P and T is still controversial; theoretical studies appeared to date have all treated POS differently, which makes the comparison of results quite challenging. When discussing theoretical findings, it is important to keep in mind that the total energy of boron decreases with occupation of the POS. Therefore, the POS should be incorporated in the calculations as completely and as realistically as possible in order to provide good approximations to the real structure.

In 2002, Zhao and Lu [51] reported the first theoretical study of α- and β-rhombohedral boron based on DFT calculations. They focused on identifying the high-pressure superconducting phase, and they did not give any detail on the phase boundary between α- and

β-boron at zero pressure. Haussermann *et al.* [40a] briefly mentioned that, in the absence of POS, α-boron is 20 meV/atom lower in energy than β-boron, but they noted that an accurate comparison must include the POS.

In 2004, Masago *et al.* [15] first reported on the relative stability of α- and β-boron, where partial occupancy was considered, although only in an approximate manner. Although the B17-B20 interstitials were ignored, these authors showed that inclusion of the B13 vacancy and B16 interstitial, in fact, reduces the internal energy of β-boron. They also calculated the Helmholtz free energies of α- and β-rhombohedral boron as the sum of the DFT total energies and the POS-configurational free energy at finite temperature. Their results indicate a transition temperature of $T_{\alpha-\beta}$=200 K under equilibrium conditions, much lower than the T at which the α–β transition was observed experimentally (1400 K). Consequently, they stated: "Taking phonon effects into account, we may obtain the calculated transformation temperature in good agreement with experiment." In 2006, the same group[3e] published a revised transition temperature, $T_{\alpha-\beta}$=970 K, with the phonon contribution added to the free energy, which was estimated from Γ-point phonons calculated with a DFT based frozen phonon method (as a reminder, the experimental transition temperatures [3b,7,26b] referred to in Ref. 3e,15 do not correspond to the ones under equilibrium conditions). In 2005, Prasad *et al.* [3d] performed DFT–total energy calculations on α- and β-rhombohedral boron, with no POS taken into account. Their results were consistent with those of previous studies: α-boron was found to be more stable than β-boron at T=0 K.

In 2007, Shang *et al.* [3h] studied the thermodynamic and mechanical stability of α- and β-rhombohedral boron using first-principles DFT total-energy and phonon calculations. They approximately took into accounts the occupations of the POS, and they also considered four different atomic densities: 104, 105, 106, and 111 atoms per rhombohedral cell. Their DFT–total

energy results were consistent with previous work: α-boron was found to be the stable phase at low temperature, and β-boron the stable one at high temperature. Shang *et al.* also pointed out that β-boron without any defects, or POS, is mechanically unstable at high temperature, although it is thermodynamically stable. They argued that introducing defects, as detected in real samples, improves on the mechanical stability. The total energy of β-boron as a function of atomic density indicates that the minimum atomic density is obtained for 105–110 atoms per rhombohedral cell. In 2009, Siberchcot [52] studied the equation of state of α- and β-rhombohedral boron using DFT–total energy calculations, where β-boron was modeled with 105 and 106 atoms per rhombohedral cell. The model with 106 atoms produced results closer to experiments. In addition, at 0 GPa, the total energy of the 106-atom model of β-boron was 4 meV/atom higher in energy than that of the α-rhombohedral phase; the zero point–motion energy (ZPE) was not taken into account.

In 2007, van Setten *et al.* [3f] reported the first theoretical DFT study on β-rhombohedral boron at the experimental atomic density, where all of the POS discovered by Slack *et al.* [8c] were considered. Starting with 106 atoms per unit cell, they studied several stable-occupation configurations. They found that a B19 occupation next to a B13 vacancy gives rise to one of the most stable structures at this atomic density; based on this information, they constructed the occupations of the POS with 320 atoms per hexagonal cell. With 106 atoms per unit cell, the most stable configuration included a B16 occupied site and no B13 vacancy; at 320 atoms per hexagonal cell the occupation configuration containing a B19-B13 interstitial vacancy–pair configuration is the most stable. Moreover, those two configurations have essentially the same total energy per atom. Van Setten *et al.* further optimized the cell parameters of the stable 106-atoms system, which brought the total energy of β-boron 1 meV/atom above that of α-boron. They also calculated the phonon density of states of α- and β-boron using the frozen phonon

technique, and estimated the quantum ZPE. When added to the total energy, one finds that the free energy of β-boron is lower than that of α-boron. Van Setten *et al.* also estimated the configurational free energy of POS in β-boron and compared the Helmholtz free energies of α- and β-boron, concluding that at 0 GPa, the β-rhombohedral phase is the thermodynamically stable phase of elemental boron at all temperatures below the melting point.

In 2008, Widom and Mihalkovic[3i] reported on yet another ground state–POS structure of β-rhombohedral boron based on DFT–total energy calculations. Their results agree with those of van Setten *et al.* on the thermodynamic stability of β-rhombohedral boron, but they disagree on the most stable POS-occupation configuration. Widom and Mihalkovic proposed that the ground state of β-boron should have a unique and ordered occupation of POS that does not violate the third law of thermodynamics, and they predicted a superlattice structure of POS. In their search for the optimal configuration, they started from systems with 107 atoms in the rhombohedral cell and built superlattice structures with systems containing 320 atoms in the hexagonal cell. Contrary to van Setten *et al.*, the stable POS-occupation configurations found by Widom and Mihalkovic consisted of the occupation of a B17-B18 pair next to a B13 vacancy pair. They also calculated the POS configuration's specific heat and the entropy of the solid as a function of temperature, which revealed a peculiar result: There was no clear sign of a first-order transition from the high-temperature, disordered configuration to a low-temperature, ordered one. Such a transition must exist to attain an ordered, ground-state POS configuration. It should be noted that such a phase transition has never been detected in measured specific heat [53] data.

In 2009, Ogitsu *et al.*[3k] reported the first results of a global–phase space search of POS-configurations in β–rhombohedral boron. We remind the reader that the astronomical number of

possible ways to occupy the POS poses one of the greatest challenges for theoretical studies of the properties of β-rhombohedral boron. For example, within the hexagonal cell, there are $\begin{bmatrix} 126 \\ 23 \end{bmatrix}$ possible POS-occupation configurations;[3k] therefore, it is impossible to conduct a thorough study based on the "hand picking" strategy used in Refs. 3f,3i.

Using Cluster Expansion (CE) techniques and DFT total energy calculations, Ogitsu, *et al*. self-consistently derived a model Hamiltonian,[51,54] and performed a global–phase space search of the POS-occupation configurations. They found many POS configurations with nearly the same total energy (nearly degenerate) that are more stable than α-boron (see Figure 12). Each of those configurations contained POS types found in previous work, namely B13-B19 vacancy-interstitial pairs and B13-B13-B17-B18 vacancy-vacancy-interstitial-interstitial pairs. In addition, a B13-B20 vacancy-interstitial pair was found in certain configurations. Most interestingly, no long-range ordering was observed in any of the stable POS configurations found in the optimization.

The most important result we want to emphasize in this section is that β-rhombohedral boron has the lowest DFT energy among all the other allotropes and polymorphs considered so far, if all of the POS found by Slack *et al.* [8c] are taken into account and the occupation configurations are optimized appropriately, at the experimental atomic density, 320 atoms per hexagonal cell. [3f,3i,3k] Therefore, β-rhombohedral boron is likely to be the ground state of elemental boron, and it is likely to be the stable phase at ambient pressure for all temperatures below melting. We note that all of the quasi-degenerate stable structures found in aforementioned calculations[3k] exhibit short-range vacancy-interstitial correlations.

As mentioned earlier, based on a linear extrapolation of the high pressure and temperature experimental results, Parakhonskiy *et al.* have recently proposed[55] that α-boron

becomes more stable than β-boron below T=933(50) K. Ogitsu and Schwegler pointed out that[56] the α–β phase boundary obtained from DFT simulation results [3k,l] is in reasonable agreement with the Parakhonskiy *et al.*'s coexistence line, within the experimental uncertainty, if one takes into account that phonon frequencies computed in the absence of POS are likely an underestimate of those of the real material.[56] In addition we note that a recent study of the specific heat of α- and β-boron combined with the heat of transformation from α- to β–boron published in 2005 [48] lead to a tentative conclusion that β-boron is thermodynamically stable at all temperature below melting. [53e]

In the next section, we describe the Cluster expansion (CE) model Hamiltonian developed in Ref. 3k, which led to the finding of a nearly degenerate ground state in β–boron.

V. Geometrical frustration in β-rhombohedral boron

The general form of a CE Hamiltonian is:

$$H = C + \sum_i U_i S_i + \sum_{i,j} J_{i,j} S_i S_j + \sum_{i,j,k} T_{i,j,k} S_i S_j S_k \cdots \quad \text{Eq. 1}$$

where C, U_i, $J_{i,j}$, $T_{i,j,k}$ are interaction parameters; when expressing the internal energy of a binary alloy, S_i takes two values, –1 or 1, corresponding to the two elements in the alloy at the crystal lattice site i. When applying Eq. 1 to the description of POS occupation of β-rhombohedral boron, the two values of S_i, –1 or 1, correspond to unoccupied (vacancy) or occupied (interstitial) sites, respectively. The highest order–interaction term considered in Ref. 3k was a three-body term that was limited to a B13-B13-B13 interaction within an individual B_{28}

unit. For the pair-interaction term, a cutoff radius of 3.5Å was selected, which is slightly larger than the second nearest neighbor distance.

Ogitsu *et al.*[3k] used systems consisting of 105, 106, and 107 atoms in the rhombohedral cell and generated 2,591 independent configurations to fit the interaction parameters, C, U_i, $J_{i,j}$, and $T_{i,j,k}$ to DFT total energies. Using these parameters, a Hamiltonian for a supercell composed of 1,280 atoms was constructed, and Monte Carlo–simulated annealing cycles were performed; then DFT structural optimizations of the atomic positions and the cell parameters of the resulting POS structures were carried out, and the optimized total energies were used to improve the CE Hamiltonian. Two fitting cycles provided a series of POS–occupation configurations, as shown in Figure 13. The discrepancy between the DFT total energies and CE energies was less than a few meV/atom.

Interestingly, if the Hamiltonian is constructed with only a pair interaction, J, it reduces to a spin Ising model. For this reason, a CE Hamiltonian is sometimes called a generalized Ising model. The CE boron Hamiltonian provides an analogy between the partial occupancy in β-boron and spin magnetism, and the interstitial-vacancy correlation in β-boron corresponds to the anti-ferromagnetic (AF) correlation in spin magnetism. Remarkably, the POS problem of β-boron is found to be well described by an AF spin Ising model!

In 2010, Ogitsu *et al.* [3l] identified an underlying model of the defects (POS) configurations of β-boron, which showed that the POS form a quasi two-dimensional network consisting of two layers of an expanded kagome lattice.[57] This discovery is crucial in understanding the observed near degeneracy in the occupation of POS in β-boron. The expanded kagome lattice—sometimes called a star lattice—is based on a hexagonal lattice with its corners

decorated with triangles (see Figure 1-d of Ref. 3l). When these triangles are expanded and their corners touch, the lattice geometry becomes that of a kagome lattice (see Figure 2 of Ref. 3l).

For some Ising models, [58] exact solutions have been found, and some of them are known to have unique properties: An exactly degenerate and disordered ground state with a macroscopic amount of residual entropy due to geometrical frustration, which is, in essence, conflict between interaction and lattice geometry. We remind readers that the AF Ising model on a square lattice has a checkerboard-type ordered ground state. Examples of geometrical frustration include AF Ising models on a triangle lattice [59] and on a kagome lattice. [60] The essence of ground-state degeneracy is often explained using three Ising spins at the corners of a triangle interacting via an AF–nearest neighbor interaction.

In the following, unless otherwise noted, we limit the range of the interaction to nearest-neighbor sites for simplicity.

We denote the Ising Hamiltonian by:

$$H = \sum_{i,j} J S_i S_j \qquad \text{Eq. 2}$$

S_i denotes the spin state at the site i, and it takes values of 1 or –1. J is the interaction parameter. When $J > 0$, an AF pair will provide an energy $J\times(1)\times(-1)=-J$. On a triangle, once an AF pair is formed, the total energy (E) does not depend on the state of the third spin. For example, with a configuration up-down-down, $E=-J-J+J=-J$, and with up-down-up, $E=-J+J-J=-J$. This system has a degenerate ground state.

A remarkable property is that, as the lattice size grows, the number of energetically equivalent configurations grows exponentially. Therefore, the entropy of the system described by Eq. 2 has a finite value at 0 K. Note that if the number of degenerate configurations does not grow exponentially, the entropy of a macroscopic system will vanish even in the presence of degeneracy. For an AF Ising model on a triangle lattice or a kagome lattice, the entropy *S(T=0K)* is 0.323 R [59b,59d] and 0.5 R [60], respectively, where *R* is the gas constant. Triangular and kagome lattices do not exhibit a phase transition, and their spin configuration is always disordered, regardless of the temperature.

In Ref. 3l it was shown that an arbitrary ground-state configuration of an AF Ising model on a kagome lattice can be mapped onto that of an AF Ising model on an expanded kagome lattice. It was also shown that the POS-occupation Hamiltonian of β-boron—a nearest neighbor AF Ising Hamiltonian on an expanded kagome lattice—possesses geometrical frustration. This model does not exhibit a phase transition, and the solution is completely disordered at all temperatures.

The CE Hamiltonian that describes the POS-occupation configuration of β-boron is substantially more complicated than the simplest form used in Eq. 2 [3k,l] (hereafter called the β-boron Ising model Hamiltonian). The Hamiltonian includes 40 interaction parameters, a complex lattice geometry, and two layers of expanded kagome lattices connected via an inverted pair of B_{28}'s. Consequently, the properties of the simple Ising model that are inherited in the β-boron Ising model Hamiltonian are not immediately apparent, but appropriate groupings of the POS elucidates the nature of geometrical frustration in this system. [3l]

The relative occupation rates of POS and their total energies obtained from self-consistent optimization cycles using CEMC and DFT–total energy calculations were somewhat surprising. [3k] First, the calculations suggested many nearly degenerate POS-occupation configurations, with no favored long-range order when using a supercell containing 1,280 boron atoms (2x2x3 of the rhombohedral unit-cell). Second, the relative occupation rates vary across a wide range but with a small energy change. Third, occupations of either a B17-B18 pairing or B19 alone are not particularly favored. Instead, these occupations almost always appeared simultaneously in a single supercell calculation. Therefore, on average, the number of B17-B18 pairs is smaller than one per rhombohedral cell, which is reflected in the concentration of holes being less than one in the electronic structure of the rhombohedral cell. The low-energy structures had well defined band gaps, with an E_g=0.8eV in the lowest one, which is in good agreement with experiments when the underestimate of the band gap due to the LDA is taken into account. Moreover, the number of observed hole states in the low-energy structures was always the same as the number of B17-B18 pairs, when the favored short-range correlations were fully developed, which supports the hypothesis that the local rehybridization around the interstitial POS dictates β-boron electronic requirements.

Clearly boron's preference for 3c2e bonds[3k,11b,c] plays a crucial role in stabilizing β-boron. One interesting question that arises in trying to understand POS geometrical arrangements is the followings: Why do POS form a 2D and not a 3D network? β-boron has many ring-type interconnections between its building units, B_{12} and B_{28}. As we discussed earlier, the hexagonal ring–type interconnections occur between interstitial sites, leading to perfect self-doping via the conversion of 2c2e bonds to 3c2e bonds; therefore, one might speculate that interstitials are the preferred POS. Very interestingly, not all of the hexagonal rings are occupied, and in the

hexagonal ring the POS occur approximately within an X-Y plane at z=0 and z=c/2, thereby making a quasi two-dimensional network (see Figure 11 and 15). If these locations within two-dimensional planes were not favored over the rest of hexagonal rings, the POS network would not form a double layer–expanded kagome lattice. Instead, it would form a three-dimensional network (see Figure 15).

The two-dimensional POS network probably arises because of the role played by the self-interstitials, B17-B20, that saturate the dangling bonds created by B13 vacancies. The other hexagonal rings—located far from the B13 sites (red hexagons in Figure 15 marked *A*, which connect two B_{12}s and a B_{28})—would not efficiently saturate the dangling bonds (see Figure 21 and 22). Therefore the B13-vacancy formation, whose mechanism Tillard-Charbonnel *et al.* [14a] rationalized, is a crucial component of geometrical frustration in elemental boron.

A crucial role is also played by B16 sites. As a few reports discussed, occupation at B16 compensates for the electron deficiency of the B_{12} icosahedra, and counters the imbalance of electron deficiency between B_{12} and B_{28}. [3k,13a] In addition to the B16 sites, the bottom of a pyramid made of four B_{12}s (see the red hexagon labeled *BP* in the lower right part of Figure 16) could also connect the B_{12}s. The B16s are located at the side of a pyramid, and they form a triangle in the X-Y plane. If the bottom of the pyramid (*BP*) were occupied, the POS network would not be an expanded kagome lattice. It remains unclear why B16 can be occupied but *BP* is not. Nonetheless, B16 occupation is consistent with the fact that the B19-B16 interaction is repulsive (AF), because the distance between the *BP* site and the closest B19 is smaller than that of the favored B19-B16 occupation configuration, where a B16 is occupied on one of the far sides of an occupied B19 triangle (see Figure 16). From these observations, it seems reasonable

to assume that occupying the far side of B16 (as compared to the *BP* site) provides a more homogeneous charge distribution, which makes the system more stable.

A. Specific heat and entropy of β-boron

In order to understand the consequences of geometrical frustration on the entropy of boron, Ogitsu *et al.*[31] performed replica Exchange Monte Carlo simulations on the β-boron Ising model for a wide range of temperatures, from below 1K to 10^8 K, and calculated the constant volume–specific heat as a function of temperature. The entropy of this model as a function of temperature was calculated by standard thermodynamic integration, where infinite temperature was chosen as the reference:

$$S(T) = S(T=\infty) + \int_T^\infty dT' \frac{C(T')}{T'} \qquad \text{Eq. 3}$$

These numerical simulations confirmed that the β-boron Ising model Hamiltonian does not show a phase transition at any temperature, and the POS-occupation configurations are completely disordered at all temperatures under equilibrium conditions.

In real β-boron samples, X-ray diffraction measurements show no long-range ordering or any sign of a structural phase transition in the occupations of the POS. Therefore, one might be tempted to conclude that the thermodynamic properties of the frustrated β-boron Ising model would explain the nature of the occupation of the POS in β-boron, but the following observation adds a twist. When Slack *et al.* [8c] performed X-ray structural analysis, they used three samples that had been left at ambient conditions for long periods of time: roughly 2, 5, and 17 years. In spite of such a long "annealing" time, those samples showed a small yet measureable difference in the relative POS-occupation rates, indicating that the relaxation time scale of self-interstitials is extremely long, and thus the configurational specific heat is very difficult to measure.

Specific-heat measurements are the most direct experimental methods to study the nature of geometrical frustration, because they reflect the number of states accessible at a given temperature. Even at low temperature, a macroscopic number of states exists in a system with geometrical frustration. For a solid, the measured specific heat consists of a phonon, configurational and an electronic contribution. Since β-boron is known to be a semiconductor, one can ignore the electronic contribution. Therefore, by subtracting the vibrational contribution from the total specific heat, one can obtain the configurational specific heat. Figure 17 depicts the configurational specific heat and the entropy of β-boron as a function of temperature. The figure also shows the total specific heat—the sum of the lattice-phonon contribution and the POS-configurational contribution—along with experimental values. The overall agreement between the experiments and the theory is excellent, but the contribution from the POS configuration is very small compared to the lattice-phonon one; the available experimental data do not permit to establish whether the configurational contribution is observed in the measured specific heat.

VI. Electronic structure of β-rhombohedral boron

In this section, we discuss the electronic structure of β-boron, particularly in relation to the stable POS occupation configuration presented in the previous section. We first offer a simplified explanation and then give a detailed analysis.

As mentioned earlier, boron displays a p-type semiconducting electronic property [9,61] with an optical-excitation gap of 1.4–1.6eV. [8c,10,62] A semiconductor-like band structure persists in β-rhombohedral boron when POS are not included, however, the valence bands are not fully occupied. The number of hole states is 15 per hexagonal cell (three times the rhombohedral unit

cell); they could be filled if one added 5 boron atoms to the hexagonal cell. In fact, the experimentally determined atomic density of β-boron, 320 atoms-per-hexagonal-cell, contains 5 atoms more than those of a cell without POS, 315 per hexagonal cell. However, it is known that the number of interstitial atoms per cell in β-boron is more than 5 since B_{28} units show a significant amount of vacancies at B13 sites. Surprisingly, neither an introduction of B13 vacancies, nor an introduction of interstitials alter the number of valence states except for one case, that is if sites B17-B18 are occupied, which introduces an additional valence state per pair. The tendency of boron to form 3c-2e bonds plays a crucial role in preserving the number of valence states upon introduction of interstitials. [3k]

The interstitial sites in β-boron act as almost perfect self-dopants. Consequently, at the atomic density of 320 atoms per hexagonal cell, β-boron becomes a p-type semiconductor. The hole states responsible for the p-type character originates from the B17-B18 pair occupation.

We note that, most likely, the following observations[63] are indirect evidence of the stabilization mechanisms of β-boron via POS occupation. It was reported in 2012 that n-type doping of β-boron is compensated by a change of POS occupation such that a semiconductor-to-metal transition is prevented,[63d] and similar phenomena have been known for some time.[63a-c]

In the following, we give more details about boron's electronic structure, including a historical perspective. Note that the electron-counting rules commonly used in borane and boride chemistry are not discussed here, but review articles are available[21,64] that cover the topic. Instead, the concept of Maximally Localized Wannier Functions (MLWF) will be used to analyze to chemical bonding.

A. The electronic requirement of β-boron without POS rationalized with B_{12} and B_{28} clusters

We first consider the preference of boron to form icosahedra, clusters made of 12 boron atoms. [4b,12] Note that a B_{12} icosahedra cluster is not stable as an isolated form, because a closed shell–electronic structure may be obtained only when external bonds are formed. Most interestingly, if all of the external bonds are 2c2e bonds, this unit lacks 2 electrons to be a perfect closed shell–electronic structure, which suggests that a B_{12} boron icosahedron might display an anionic character in the condensed phase. [4b] The counter part, a cation-like boron cluster, can be realized in the triply fused icosahedron, B_{28}, which has an excess number of electrons for the number of chemical bonds involved[14a,65] (see Figure 18).

In 1955, Longuet-Higgins and Roberts rationalized the electronic requirements of boron icosahedra. [4b] Based on MO theory, they concluded that $B_{12}H_{12}$ has an open shell–electronic structure; therefore, it is not stable as a neutral molecule. They suggested that an ion, $B_{12}H_{12}^{-2}$, might exist. Evarhardt, Crawford, and Lipscomb reached a similar conclusion.[11a] Five years later, Pitochelli and Hawthorne synthesized $K^{+2}(B_{12}H_{12})^{-2}$, which confirmed that $B_{12}H_{12}^{-2}$ is indeed stable.[12] The electronic structure of the B_{28} cluster unit was not fully understood until 2000 (see Figure 19).[14a]

The electronic structure of the triply fused icosahedra, the B_{28} unit, was explained through extensive research on intermetallic compounds, such as $K_4Na_{13}Ga_{49.57}$, [14a,45a,45d-g,66] in which an isostructural cluster unit—the triply fused icosahedra made of gallium atoms $(2Ga_{28})Ga$—forms. A description of Ga clusters found in intermetallic compounds helps to understand B_{28} in boron. In a subgroup of these compounds, namely p-block intermetallic–Zintl phase compounds, the charge transfer from low-Z metals to a p-bock element such as gallium is

supposed to be complete. Therefore, one may deduce the charge state of the cluster in the compound form, and a very similar stoichiometry is found in some salts, such as $K^{+}_{2}B_{12}H_{12}^{-2}$. [12]

Extended Huckel calculations on an isolated $Ga_{28}H_{18}$ cluster showed that, when the external bonds of Ga_{28} are completed with 2c2e bonds they have more than enough electrons to fill out the bonding orbitals, which means that the triply fused icosahedra, Ga_{28}, are cationic. Therefore, they are unlikely to be present in pure form in a Zintl phase–intermetallic compound in a reducing environment. Interestingly, the triply fused icosahedra in those compounds have vacancies at the atomic sites corresponding to the B13 vacancy site in a B_{28} unit of β-rhombohedral boron. [14a] The local/global bonding/anti-bonding character of an electronic state associated with this vacancy site in Ga_{28} was analyzed using a crystal orbital overlap population (COOP) approach or its molecular version, MOOP, which showed the following. [14a] First, without the vacancies corresponding to B13, the valence electrons will occupy globally anti-bonding electronic states. Second, the vacancy sites are in a triangular configuration, and the HOMO band has locally anti-bonding character within the triangle. These sites have globally bonding character, such as that between B13 and its surrounding atoms. Removal of a vacancy atom does not change the number of bonding states in Ga_{28}; therefore, an introduction of a vacancy at this site lowers the Fermi level of the system and reduces frustration by removing the local anti-bonding orbital. Unfortunately, studies of Zintl phases did not confirm a precise electron count for $(2Ga_{28})Ga$ because those intermetallic compounds tend to have additional vacancies, which makes it difficult to compare the theoretical electron count and the experimental value estimated from the material's stoichiometry. Nevertheless, a qualitative explanation exists: Perfect Ga_{28} will have an excess of electrons occupying global/local anti-bonding orbitals, which appear around the bottom of the conduction band, and the introduction

of vacancies at the B13 sites will stabilize the system by not occupying the global anti-bonding orbitals and by removing the local anti-bonding orbitals close to the top of the valence band. In 2001, Jemmis and Balakrishnarajan [65] confirmed an accurate electron count for $(2B_{28})B$ based on a combination of an empirical electron-counting rule and MO cluster calculations. When all of the external 2c2e bonds are formed, $(2B_{28})B$ has three more electrons than needed for a closed-shell structure. There are effectively four B_{12} units in a unit-cell of β-boron, which lack two electrons to be a closed shell, and that makes a total of eight electrons short per cell for the icosahedra. With one $(2B_{28})B$ unit per rhombohedral cell, the total electron count for β-rhombohedral boron without partial occupancy is $-8+3=-5$ relative to a closed shell, which is in perfect agreement with an earlier estimate based on bulk-phase, electronic band–structure calculations (see Figure18). Jemmis and Balakrishnarajan also showed that one vacancy per B_{28} unit at B13 lowers the total energy of an isolated $(2B_{28})BH_{36}$ cluster (to be precise it should be $(B_{27})B(B_{28})H_{36}$ or $(2B_{27})BH_{36}$), where the electron requirements, or the number of bonding orbitals, do not change by introducing a vacancy at the B13 site. These researchers also proposed that since B_{12} and B_{28} have opposite ionic characters, moving a B13 atom to a B16 interstitial site may reconcile the imbalance in the electron requirements (or ionicity), since B16 sites are surrounded by B_{12} icosahedra. They further suggested that five additional atoms per hexagonal cell occupying the POS identified by Slack *et al.* [8c] will make β-rhombohedral boron a closed shell–electronic structure. Note that five atoms per hexagonal cell correspond to 5/3 atoms per rhombohedral cell, which add exactly five electrons per rhombohedral cell. The discrepancy between the experimental observation of β-boron being semiconducting and earlier theoretical work [8b] seemed to have been reconciled, despite the lack of an explanation for why the additional self-interstitials do not change the number of valence states per unit-cell. The work of Ref. 13a

did not discuss whether partial occupancy is purely an entropic effect at high temperatures or if its occurrence lowers the internal energy of the solid.

The first theoretical electronic-band structure calculation on β-boron, without taking partial occupancy into account, was published in 1982, [8b] and it suggested an incomplete valence band—five electrons per rhombohedral cell short of a closed-shell structure. Such an insufficient number of valence electrons should generate a metallic character rather than a semiconducting one. Most importantly, such a crystal structure would be unstable because of the incomplete formation of chemical bonds, which seemed to have been the case with the T-50 allotrope. Bullett [8b] suggested that the disorder reported experimentally, e.g. the presence of partial occupancy, might be at the origin of the discrepancy between the experimental observations and the early theoretical calculations of the electronic requirement (i.e., a stable allotrope should have a closed shell–electronic structure). [8b]

B. DFT simulations begin to explain the nature of POS

In 2002, Imai *et al.* [67] reported the first electronic band structure of β-boron with POS, based on DFT; the precise locations of the atoms with POS for their three β-boron models are not available.

As mentioned before, in 2007, van Setten *et al.* [3f] showed that a B19 occupied site near a B13 vacancy significantly reduces the internal energy of β-boron, because it yields a nearly closed shell–electronic structure, but the band gap, E_g=0.35eV, is significantly smaller than the experimental value, about E_g=1.5eV, even considering the well-known underestimate due to the approximation used for the exchange-correlation energy.

In 2008, Widom and Mihalkovic [3i] found a different stable structure based on B17 and B18 occupations next to a B13 vacancy pair. Their band structure has one hole state per rhombohedral cell with E_g~0.8eV, which is in better agreement with experiments. In Ref. 3f,3i, the mechanism that keeps the number of valence states almost constant was not described.

In 2009, Ogitsu *et al.*[3k] studied the local bonding properties of the configurations identified by their CEMC search, by using Maximally Localized Wannier Functions (MLWF) and showed two types of rehybridization mechanisms: One keeps the number of valence states unchanged and the other introduces an additional valence state (see Figure 20–22).

We note that to rationalize the chemical bonding in borane and boride, researchers have developed many types of electron-counting rules.[65,68] Those approaches were very powerful tools for rationalizing or predicting the stable forms of boron clusters. However in β-boron, POS are located at the links between the cluster units, so the separation into fragments with uniquely defined electron counts faces great challenges. This is why an alternative approach based on MLWFs, which is better suited for describing condensed phases,[3k] was adopted.

The MLWFs are related to the eigenfunctions of Kohn-Sham orbitals—the solution of the DFT Hamiltonian—by a unitary transformation, where the unitary matrix is defined so as to minimize the sum of the spreads of the transformed functions (Wannier Functions).[69] Note that conventional Wannier Functions are expressed as the Fourier transformation of the Bloch states, where each function is localized within the primitive unit-cell. Upon successful "maximal localization," one might often relate a MLWF to a chemical bond based on the location of the center of the MLWF and its spread. Therefore MLWFs generalize the concept of Boys orbitals used in quantum chemistry.[70] A MLWF is "occupied" by two electrons when it is constructed

from the occupied Bloch states, and when spin degeneracy is assumed. When a MLWF appears to be well localized between two atoms, it is natural to assume that a 2c2e-type covalent bond is formed. This is the case in diamond and silicon where each MLWF is localized at one of four sp^3 covalent bonds. Therefore, given the locations of the centers of MLWFs and the spreads in diamond and silicon, one can unambiguously identify the types of bonding configurations in these systems. [3k] A 3c2e bond of boron can be described as a bonding orbital consisting of a linear combination of three atomic orbitals, where the bonding charge is concentrated at the center of three atoms.

When the bonding orbital becomes delocalized and the number of bonds in a system becomes incommensurate with its geometrical feature (such as the number of edges and/or the number of faces of the cluster) the bonding-property information from the MLWFs is limited, perhaps, reflecting the full quantum mechanical nature of chemical bonding. In this case, the number of bonding electrons can still be estimated from the MLWFs, but an individual MLWF cannot be interpreted as a unique chemical bond. For example, a $B_{12}H_{12}$ cluster has 13 intra-cluster bonding orbitals, a number that is incommensurate with the 30 edges and/or 20 faces.[4b,11a] Those bonding orbitals are delocalized over the cluster, and sometimes interpreted as metallic bonds.

In bulk β-rhombohedral boron, the number of MLWFs belonging to a B_{12} is 13, which is in agreement with empirical electron-counting rules. [3k] Here the criterion for "belonging to a B_{12}" are so defined: The centers of MLWFs are located inside the polyhedron defined by the planes that are normal to the vertices of the B_{12} and passing through the corner of B_{12}. We note that the electron count for $(2B_{28})B$ in bulk β-boron obtained from MLWF was confirmed [3k] to be

in agreement with the results of Jemmis *et al.,* [65] who used an empirical electron-counting rule and MO calculations on the $(2B_{28})B$ cluster fragment.

The main results from a MLWF analysis are the following. When the centers of hexagonal rings (B16, B19, and B20) are occupied, three 2c2e bonds are converted to three 3c2e bonds, but the number of bonding states does not change (see Figure 20 and 21). Boron's preference for 3c2e bonds[3k,11b,c] plays a crucial role in stabilizing β-boron. On the other hand, when B17 and B18 are occupied in a paired configuration, the number of bonding states increases by one (see Figure 22). The B17-B20 occupations saturate the dangling bonds in the B_{28} unit created by the B13 vacancy, thus favoring the locations close to B13 (see Figure 21 and 22). The occupation of the hexagonal-ring site leads to perfect self-doping. The three electrons per boron atom increase the energy of the Fermi level without changing the number of valence bands, and at the experimental atomic density—320 atoms per hexagonal cell—β-boron should become a closed shell–electronic structure system. On the other hand, a B17-B18 pair occupation introduces an additional valence band, promoting a hole state. Therefore, it is important to determine the optimal relative occupation rates between B17, B18, and B19 (or B20) to make comparisons with the experimental observations of a p-type semiconducting character [9,61] with a very low conductivity and an optical gap of about 1.5 eV. [8c,10,62]

In summary, the electron counts for B_{12}[4b,12] and $(2B_{28})B$[13a,14a] estimated from the cluster-fragment approach are not altered in the bulk phase.[3k,8b] The introduction of a B13 vacancy does not change the electron count for B_{28}.[13a,14a] Consequently, β-boron, without POS, has an insufficient number of valence electrons—five electrons per rhombohedral cell—for a closed shell–electronic structure. These results[3k] are in agreement with the proposed electron counts of β-boron using the cluster fragments and older electronic–band structure calculations.[8b]

C. Atomic density and favored POS configurations: What are the implications?

As we discussed in the previous section, the stable B19 occupation does not change the electron count, and a B17-B18 occupation increases the number of bonding orbitals (or valence bands) by one. [3k] As a consequence, the relative stability of these two occupation configurations depends on the chemical potential of the system, since they have a different number of bonding orbitals. At a lower atomic density, the system has fewer valence electrons, thus favoring a B19 occupation over a B17-B18 occupation;[3f] the opposite preference arises at the higher atomic density. [3i]

The occupancy of the B13 site also impacts the structure of other units in β-boron. For example, if the Fermi level is low enough so that the HOMO-LUMO orbitals of the B_{28} cluster unit (which have local anti-bonding character) are not occupied (see Figure 19), then the B13 site is occupied. In that case, the nearby B17-B20 interstitials, which serve to terminate the dangling bonds created by a B13 vacancy, are not present either. Accordingly, B17-B20 occupations are not the most favorable structure in the 106-atoms systems, while the B19 occupation becomes the most stable since it forms the closed shell–electronic structure at the experimental atomic density, 106 2/3 atoms per rhombohedral cell.[3f]

The atomic density affects the density of the B13 vacancies via the location of the Fermi level with respect to the HOMO-LUMO levels of B_{28}, which in turn dictate the B17-B20 occupations. [3k]

These considerations lead to an interesting hypothetical situation: If B_{28} did not exhibit a local intrinsic instability at the B13 site, β-rhombohedral boron could have been a stable and electron-precise semiconductor with only one type of POS, B16, at the atomic density of 320 atoms per hexagonal site; indeed the presence of a B16 occupation leads to perfect self-doping

by converting the bonding from 2c2e to 3c2e. Therefore, the local frustration within the B_{28} unit apparently contributes to the complexity of β-rhombohedral boron.

Another interesting aspect of the stable occupation of the POS is that the *ab-initio*/CEMC optimization procedure resulted in the persistent presence of B17-B18 pair occupations. This increases the number of valence bands, leading to a small amount of hole states, which prevents these bands from being perfectly electron precise. [3k] If the true ground-state POS configuration of β-boron is required to be electron precise—a perfect semiconductor—the atomic density must be slightly higher than 320 atoms per hexagonal cell.

VII. Anomalous properties of β-rhombohedral boron

Many experimental studies have reported that β-boron exhibits anomalous transport and optical properties.

Tsagareishvili *et al.* [18a] performed internal-friction experiments for a wide range of temperatures and reported the most direct evidence of diffusion of boron defects. They measured the inelastic response of the system during periodical distortions. The origin of an inelastic response is usually interpreted as originating from defect diffusion, which dissipates energy. In Ref. 18a clear peaks are reported at temperatures of 150K and 530K. The activation energies, E_a, for those peaks were determined from their temperature dependencies, E_a=0.13 eV and E_a=1.3 eV, respectively. The authors state that no first order–phase transition could be detected in the samples of β-rhombohedral boron by thermal or X-ray analysis. Later, they reported more peaks with some evidence that impurities might contribute to the inelastic response. [18j,71] These

experimental observations seem to support the notion of boron-defect diffusion over a wide range of temperatures.

Werheit and Franz [18l,m] reported a dramatic change in the optical absorption of β-boron within the band gap around 150–180 K. Below this temperature range, one clear absorption peak appears at E=0.4 eV above the valence-band top; above this temperature range, many trap levels appear over the entire range of the band gap. Exposure to light changes the absorption profile and the corresponding relaxation time scale was found to be very long, of the order of several hours or more at about T=100 K. Consequently, the sample had to be left in the dark for a long time before making measurements. Werheit and Franz suggested that the peculiar behavior of β-boron's optical properties may be explained by the diffusion of boron interstitials.

Lonc and Jacobsmeyer [72] measured magnetoresistance as a function of temperature and magnetic field. The results are interesting and puzzling. Single-crystal measurements show negative (positive) magnetoresistance in low (high) magnetic field. For a fixed magnetic field, the temperature dependence of the magnetization shows a peak located at ~100 K. On the other hand, polycrystalline measurements showed only positive magnetoresistance, with the same peak position of the magnetization as in the single-crystal measurements. Using optical excitation at T=77 K to set up the initial conditions of the sample, Zareba and Lubomiska [18b] measured the thermally stimulated current and observed peaks at T=117 K and 214 K. The peak at 117 K appears after a long duration of optical excitation. Geist [18g] reported on the temperature dependence of the photoconductivity and on the photo-electron paramagnetic resonance (photo-EPR); the former showed different temperature profiles at high and at low temperatures. Moreover, Geist noted that the concentration of the gap level at E=0.23 eV above the valence band top was about one state per rhombohedral cell. He also suggested that the peculiarity of his

observation might be related to the incommensurate number of electrons and bonds in β-boron. Tavadze *et al.* [18i] measured the temperature dependence of the dielectric loss at 50 Hz, and found a peak at T= 213 K with E_a=0.18 eV. They observed another peak at T=233 K with E_a=0.23 eV, which completely disappeared by annealing at T=978 K with H_2. Young, Oliver, and Slack [18c] measured the temperature and frequency dependence of microwave elastic losses, which showed a steep rise at a temperature of about 100 K. Kubler *et al.* [18e] measured the magnetic susceptibility over a wide range of temperatures and their results indicate that impurities are not likely to be responsible for the observed gap levels.

In addition, the following experimental reports might be related to boron-defect diffusion. Golikova's team measured the temperature-dependent resistivity (ρ) and found that the slope of log ρ/(1/T) changes at a temperature of about 200 K. They suggested that the conduction mechanism of β-boron is that of a Mott type–variable range hopping. [73] Moreover, the photocurrent as a function of illuminance measured at various temperatures clearly showed distinct behaviors below and above T=200 K. [74]

In 1993, Werheit, Laux, and Kuhlman [10a] reported on the detail of the optical absorption and its relaxation behavior, and from this they interpreted the anomalies observed in various physical quantities at around T=500–600 K, including the internal-friction peaks, elastoresistance, thermal expansion, electrical conductivity, thermal conductivity, and EPR. [18a,18e,f,75] Although it is not clear if all of those observations share the same origin, the POS-hopping mechanism reported in 2010 [31] might be responsible for some of the anomalies, but further investigations are needed to come to robust conclusions.

In 2004, Werheit and Wehmoller [18n] reported on the stochastic jumping behavior of the time dependence of the dc conductivity and the photoconductivity, and they attributed those

observations to boron-defect diffusion. In 2009, Werheit and Kummer [76] described fractional photoconductivity glow experiments and argued that their results support the notion of optically induced structural changes in the POS. In 2012, the specific heat of β-boron measured by differential scanning calorimetry was reported.[77] Based on these results, it was suggested that B13 atoms may start to diffuse at about T=550 K. The estimate of Ref 77 on the activation barrier, E_a=4.75 eV, is consistent with theoretical values reported on B13 diffusion.[3l,77]

The other types of reported anomalies are: large capacitance, [78] the pressure effect on dc conductivity, [79] the isotope effect on the mechanical properties, [71c,80] the kink in the very low temperature specific heat, [53d] and an isotope effect on phonons that indicates non statistical isotope distribution.[81] Note that the kink in the specific heat might originate from localized Einstein phonons due to disorder in the POS; the kink in the specific heat was observed at very low T (~1 K) and is unlikely related to defect diffusion.

The most relevant explanation of the observed anomalous properties of β-boron comes from recent theoretical studies, [3k,l] which showed that the lattice of POS exhibit geometrical frustration that leads to a macroscopic amount of states near the ground state (or near degeneracy). More specifically, there are a large number of boron defects configurations, which may be dynamically explored via their diffusion even at low temperatures if the barriers separating those configurations are low enough. Ogitsu *et al.* reported that there are at least two low-activation paths: one between adjacent B16 sites and another between adjacent B19 and B20 sites, with barriers of 0.25 eV and 0.5 eV, respectively.[3l] These findings suggested that the low-temperature excitation at ~150–180 K is related to B16-B16 interstitial hopping, and the higher temperature excitations at ~500–600 K are related to B19-B20 interstitial hopping (as mentioned above, Hoffmann and Werheit suggested that this excitation is due to B13 diffusion with an

activation barrier of E_a=4.75 eV[77]). The most stable POS configurations [3k] showed a very clear band gap with a small amount of hole states in the valence bands. It was also found [31] that introducing unfavorable B16 occupation, close to B19, adds a significant amount of gap levels, although it only raises the total energy by several meV/atom. Therefore, the interstitial atoms at B16 sites could hop within B16 sites over a wide range of temperatures, and the hopping between energetically degenerate B16 sites could take place at T<150 K. At higher temperatures, the B16 interstitial might be able to hop into a B16 next to a B19 occupation or next to a B17-B18 pair, which would introduce gap levels. [31]

Finally, we note that nearly identical mechanisms underlie the near-degeneracy of β-boron defects and frustrated spin magnets, where a variety of experimental and theoretical methods have been employed to understand the nature of the problem. We suggest that approaches similar to those used for spin magnets might play a crucial role in understanding the partial occupation's effect on boron's mechanical and electronic properties under various physical conditions. For example, applying a magnetic field to a frustrated spin magnet is a powerful tool to investigate the nature of frustration. In the case of boron, changing the chemical potential of electrons corresponds to the application of a magnetic field to a spin magnet. Given that pressure changes boron's chemical potential, pressure dependent experiments might expose the nature of boron-defect diffusion. In fact, Zhang *et al.* [79] demonstrated that applying pressure to boron alters its electric conductivity and the temperature dependence of the conductivity.

VIII. Issues related to the third law of thermodynamics

In closing we remind the readers of the various versions of the third law of thermodynamics. According to Linder, [82] four forms of the third law of thermodynamics can be found in the literature:

1) The original Nernst's Heat Theorem: $\lim_{T\to 0K} \Delta S(T) = 0$

2) Planck's form: $\lim_{T\to 0K} \frac{S(T)}{N} = 0$

3) Lewis' form: "Every substance has a finite positive entropy; but at the absolute zero of temperature the entropy may become zero, and does so become in the case of perfect crystalline substances."[83]

4) Unattainability of absolute zero temperature.

Despite this variety of options, Linder states that none is "completely satisfactory from a phenomenological point of view."

Schwabl [84] formulates the third law as statements 1 and 4 with the condition that the constant value of entropy is independent of parameters, such as pressure and volume. Within this formulation, the presence of a macroscopic amount of residual entropy does not contradict the third law. Landsberg [85] provides a similar view. Gokcen and Reddy [86] state that Nerst's heat theorem is the third law, and they propose the convention of taking zero entropy as the constant value, because many experimental observations, such as the entropies of allotropes, consistently show a convergence to a unique value. Dugdale [87] presents a similar view. Kaufman [88] states that statement 4 is the third law, and he discusses how it leads to statement 3. Although none of these

textbooks describe Planck's form as the definitive third law of thermodynamics, some older references [89] do.

In 2006, Kox [90] wrote: "Nowadays it is the view of many that quantum theory provides a solid basis for the statement that at absolute zero all systems have zero entropy and that one can formulate the Third Law in this way. But others still confine themselves to the statement that one cannot reach absolute zero. In spite of these differences, however, there does seem to be a general consensus that the Third Law is of a different, less fundamental and more experimental character than the other laws of thermodynamics."

The discussion of boron given in this review is based on Planck's form, stating that a disordered and degenerate ground state with a macroscopic amount of residual entropy in a real system cannot exist. Therefore, boron's ground state must be described as "nearly" degenerate. This view arose from extensive studies on ice and spin ice. Their thermodynamic properties have been well described by a frustrated Ising model, which has an exactly degenerate and disordered ground state and is similar to the Ising model used for the POS problem in β-boron. The long and controversial studies on ice and spin ice have resulted in a tentative consensus: The presence of zero-point entropy is likely to be a non-equilibrium property.[16h] However, a different scenario has been proposed recently: A frustrated spin system may have a quantum liquid ground state with U(1) symmetry.[91] The implication of this new development in relation to the third law of thermodynamics are yet to be understood.

For convenience of the readers in understanding the controversial nature of the ground-state entropy, we briefly summarize the studies of classical frustrated systems. First, the presence of degenerate ground states is not sufficient for a system to exhibit a macroscopic amount of

residual entropy. A macroscopic amount of residual entropy requires the system to have an exponentially increasing number of degenerate–ground state configurations as a function of system size. If the scaling of the degeneracy is weaker than exponential, the zero-point entropy converges to zero in the limit of large system sizes. There are very few examples of such exponentially growing degeneracy, and ice and spin ice are the well-known cases.

In 1935, Pauling [16c] successfully explained the reported residual entropy [16b] of ice based on the proton-disorder model. [16a] An H_2O molecule has six independent proton configurations in the tetrahedral coordination of ice, and one-quarter of those have protons in the adjacent water molecules, thus satisfying the "ice rule" of Bernal and Fowler. [16a] The resulting number of configurations (W) for ice consisting of N water molecules is $W=(6/4)^N$, and the corresponding residual entropy is $S/N=R\ln 3/2\sim 0.802$ E.U. The corresponding value estimated from the available experiments [16b] was 0.87 E.U. In 1936, Giaque and Stout [16d] updated this estimate to S(T=0 K)=0.82 E.U (0.42 R) by conducting experiments that were particularly careful about the attainment of equilibrium. Their result is in very good agreement with Pauling's estimate based on the proton-disorder model. In the same year, Long and Kemp [92] reported on the residual entropy of D_2O in an attempt to discriminate the proton-disorder model from a competing theory based on ortho-para water, which predicted residual entropies for H_2O and D_2O of 1.033 and 0.459 E.U. (0.52 and 0.23 R), respectively. Their estimate—based on essentially the same procedure used by Giaque and Stout—resulted in a residual entropy of 0.77 E.U. (0.39 R), strongly supporting Pauling's hypothesis on proton disorder. Pauling suggested that the observed residual entropy "may arise either from failure of the experimenter to obtain thermodynamic equilibrium in his calorimetric measurements, or from errors in the extrapolations." [16c]

In 1982, Tajima *et al.*[93] showed that KOH-doped ice exhibits a structural phase transition at T=72 K where up to 70 percent of the residual entropy is removed, which suggests the presence of an ordered phase of ice at low temperatures. This phase was named ice XI. Given that the transition temperature does not change even with a KOH concentration diluted by two orders of magnitude, catalyzation by doping—not a modification of the phase stability upon doping—is believed to cause the observed phase transition. In 2005, Singer *et al.* [94] demonstrated—based on first-principles DFT total-energy calculations—that the ordered phase of ice XI below T=90 K has a lower free energy than that of proton-disordered ice, I_h, which is the hexagonal crystal form of ice observed at ambient pressure and right below the melting temperature. This result is in qualitative agreement with experiments.

The studies on the residual entropy of ice, continuing over seven decades, support the notion that a macroscopic amount of residual entropy at T=0 K is a non-equilibrium property due to the slow dynamics at low temperatures, and direct experimental evidence of a low-temperature ordered phase has been provided.[93,95] Also, Pauling's calculations [16c] on the residual entropy do not account for the long-range dipole-dipole interactions between water molecules, but the DFT calculations do.[94] Consequently, the residual entropy in ice is consistent with Planck's form of the third law.

Information about the macroscopic residual entropy in spin magnetic–pyrochlore materials, or spin ice, evolved much like the studies of ice during the years, but the current consensus is not as definitive because of the lack of a direct experimental discovery of an ordered phase. For spin ices, a very simple model Hamiltonian—a spin Ising model—played a crucial role in understanding the nature of the problem, that is how geometrical frustration can

lead to a degenerate and disordered ground state with macroscopic residual entropy, and how introducing long-range dipole interactions may lift the ground-state degeneracy.

The first exact solution to a one-dimensional Ising model was published in 1925. [58] In 1950, three independent groups—Wannier,[59a] Houtappel,[59c] and Husimi and Syozi [59b]—reported an exact solution of an AF Ising model on a two-dimensional triangle lattice, which does not exhibit a phase transition to a low-temperature ordered phase. The ground state of this model is exactly degenerate and disordered with a macroscopic amount of residual entropy, S(T=0 K)=0.3383 R, [59a] which was later corrected to be 0.323066 R. [59d] In the following year, Syozi [60a] demonstrated that an AF Ising model on a kagome lattice also has an exactly degenerate and disordered ground state, and in 1953, Kano and Naya [60b] reported a significantly larger residual entropy for this system, 0.50183 R. We now call these models frustrated Ising models. In 1956, Anderson [17] pointed out that an Ising model is the common underlying Hamiltonian for spin ordering and atomic ordering in ferrites and the proton-disorder problem in ice. In 1997, Harris *et al.* [16g] showed that the spin magnetism in pyrochlore, $Ho_2Ti_2O_7$, and the proton-disorder problem of ice can be mapped on a ferromagnetic Ising model on a corner-sharing tetrahedron; hence, those magnetic pyrochlore materials are called spin ices. This Ising model with nearest neighbor interaction is exactly degenerate and disordered with a macroscopic amount of residual entropy, and the measured temperature profile of the specific heat (C(T)) is in excellent agreement with that of the Ising model calculated by Monte Carlo simulations. [16h] However, by introducing more realistic, long-range dipole-dipole interactions to this model and by using a more advanced cluster update–Monte Carlo algorithm the presence of an ordered ground state was revealed, but the C(T) profile above the transition temperature is almost identical to that of an NN Ising model and the C(T) reported by experiments. [16h] Although the predicted phase

transition has never been observed by experiments, the measured short-range, spin-spin correlation from neutron-diffraction experiments agrees with a dipole Ising model, rather than an NN Ising model. [16h] This led to the consensus that the observed residual entropy in the magnetic pyrochlore materials is likely to be a non-equilibrium property caused by the slow dynamics at low temperatures. [16h] In this case, Planck's form of the third law is unlikely to be contradicted.

In the spin Ising model, spins are treated as classical degrees of freedom, and as mentioned before it was shown that a quantum mechanical description of frustrated spin magnets may have a quantum spin liquid ground state with U(1) gauge symmetry.[91]

We end this section by pointing that according to Gokcen and Reddy, [86] the observations on the S(T) of allotropes lead to the adoption of the Planck's form of the Third Law as a convention, $\lim_{T\to 0K} S(T) = 0$. As discussed here, it was established only very recently that a macroscopic amount of defects in an allotrope of boron, β-rhombohedral boron,[8c] is thermodynamically stable at low temperature,[3f,3i,3k] and the structure exhibit geometrical frustration.[3l]

IX. Prospect of boron research

Determination of the phase diagram of elemental boron has been a very active area of research, yet the location of the phase boundaries is still quite uncertain (see Figure 1). The major challenges on this subject stem from the intrinsic properties of elemental boron: Complex crystal structures of boron allotropes that are separated by large kinetic barriers[3j,5b,7] and the structural and electronic properties that have strong tendency to accommodate impurities. [4e-g,20,96] The large kinetic barrier is a serious obstacle for the experimental determination of phase

boundaries. Direct mapping of the phase boundaries in high-pressure and temperature experiments has not been successful at low pressure and temperature due to slow kinetics. [2,4n,28b,55] Use of a catalyst such as Pt might help to solve the problem, [55] however, a careful assessment of the impact such an impurity has on the thermodynamic stability of different phases will be necessary. [4e-g,20,96] A determination of the Gibbs free energy profile from calorimetric measurements could be an alternative approach, which requires large enough high quality samples[24c,d,53e,97] and an accurate estimate of the enthalpy difference between phases (heat of transformation). [48] There are a few recent developments in solving the former problem, [24c,d,53e] while the latter is still a major obstacle. Within theory, an assessment of the accuracy of approximations used in previous works, *e.g.* local or semi-local descriptions of the electronic exchange-correlation energy,[98] will be desired. A more precise yet computationally expensive method such as Quantum Monte Carlo (QMC) may be applicable even to the large boron cells thanks to rapid improvements in computing power.[99] Although QMC will be able to provide an accurate estimate of the enthalpy differences between allotropes at T=0 K, the computed phonon contribution to the free energy[100] will inevitably have some uncertainty due to the presence of POS. A combination of theory (*e.g.* QMC) and experiment (*e.g.* specific heat measurements) might be the most realistic approach applicable in the near future to enable an accurate determination of the phase diagram of boron.

Using our simple model[3k,l] that accurately describes the POS-occupation problem in β-boron, it would be interesting to pursue future investigations of the impact of POS-occupation on the various transport properties of boron. In particular, it is likely that the lack of a precise microscopic model for representing the POSs in boron has prevented researchers from fully exploiting the potential uses for boron in electronic devices.

As an analogy with spin-magnetic systems suggests, modifying the chemical potential of boron—for example, by applying pressure—might provide a way to tune the relative preference of B19 and B17-B18 occupations, which might reveal a new ordered phase. Combined with precise calorimetric measurements, this might enable fine-tuning of the electric/magnetic properties of elemental boron through partial occupations. Moreover, boron's unique photoconductance, large capacitance, and magnetoresistance might be controlled with doping, which could lead to boron-based spintronic devices. In addition, recent and rapid developments in the theory of boron-based nanomaterials—specifically in low dimensional structures—are already showcasing diverse and unique properties that might lead to novel devices.[101]

The peculiar properties that hindered the development of boron-based opto-magneto-electronic devices could become an advantage as we learn to control the properties of boron defects. Now, the door is wide open, and only a few more obstacles—all identified—must be negotiated to reach the opportunities in sight.

X. Acknowledgement

During the course of our research on boron, we discussed with many researchers, who greatly helped understanding the extraordinary nature of elemental boron: Dr. Seiji Mizuno (University of Hokkaido, Japan), Prof. Yukitoshi Motome, Dr. Masafumi Udagawa, Prof. Kaoru Kimura, Dr. Shinji Todo, Prof. Koji Fukushima, Prof. Shinji Tsuneyuki, Prof. Kazuo Ueda (University of Tokyo, Japan), Prof. Syoji Yamanaka (Hiroshima University, Japan), Dr. Takao Mori (NIMS, Japan), Prof. Mary Anne White, Mr. Anthony Cerqueira (Dalhousie University, Canada), Prof. Nicola Marzari (École Polytechnique Fédérale de Lausanne, Switzerland), Prof. Manfred Sigrist, Prof. Matthias Troyer (Eidgenössiche Technische Hochschule Zürich,

Switzerland), Dr. Jonathan Yates (Oxford University), Prof. Ivo Souza (Universidad Del Pais Vasco, Spain), Dr. Roderich Moessner (Max Planck Institute Dresden, Germany), Prof. Francois Gygi, Dr. Leonardo Spanu (University of California Davis, USA) and Dr. John Reed. TO acknowledges assistance of Liam Krauss (Lawrence Livermore National Laboratory) in generating some of figures.

Part of this work was performed under the auspices of the U.S. Department of Energy by Lawrence Livermore National Laboratory under Contract No. DE-AC52-07NA27344 and partially supported by DOE/SciDAC under Grant No. DE-FG0206ER46262.

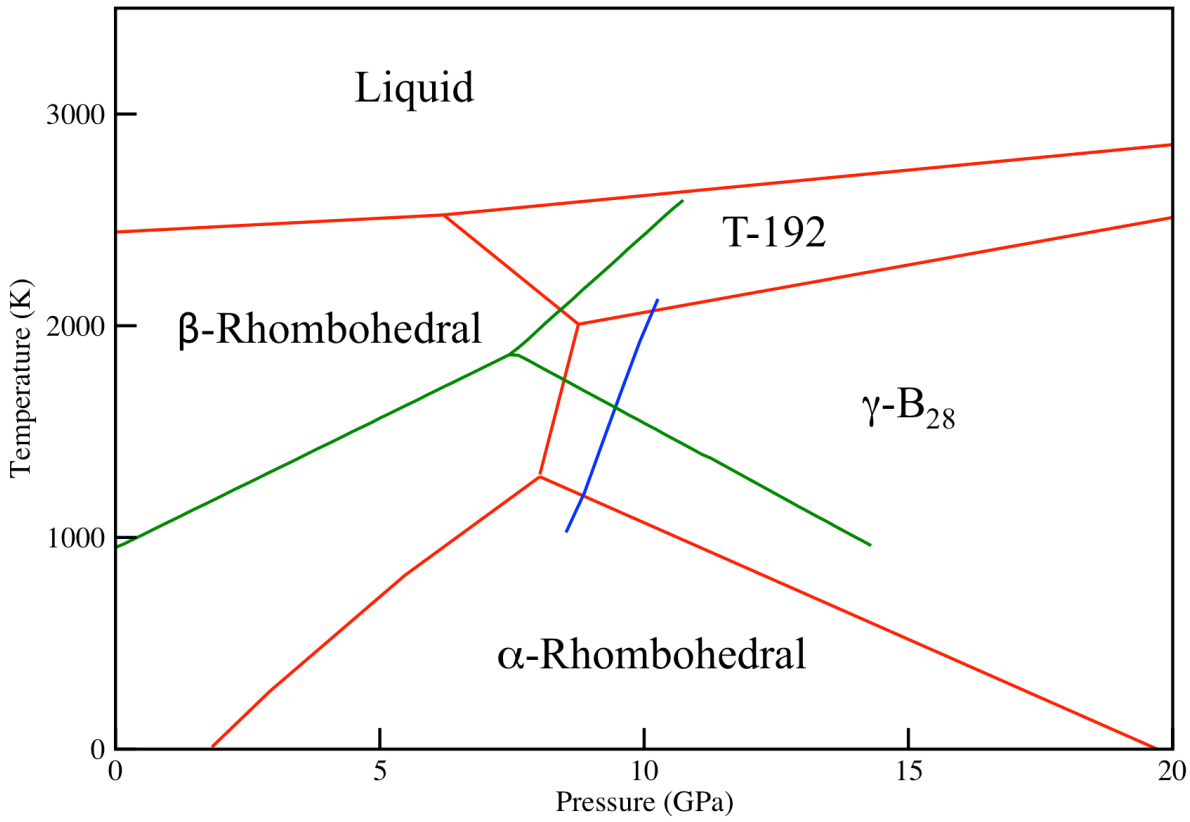

Figure 1. Phase diagram of elemental boron published in recent reports. These reports yield a consistent energy ordering of the different phases (α-boron, β-boron, γ-B_{28}, T-192) however, large uncertainties remain on the location of phase boundaries. Red lines are from Oganov *et al.* Nature **457**, 863 (2009), the blue line is from Zarechnaya *et al.* Phys. Rev. Lett. **102**, 185501 (2009) and the green lines are from Parakhonskiy *et al.* Sci. Rep. **1**, 96 (2011).

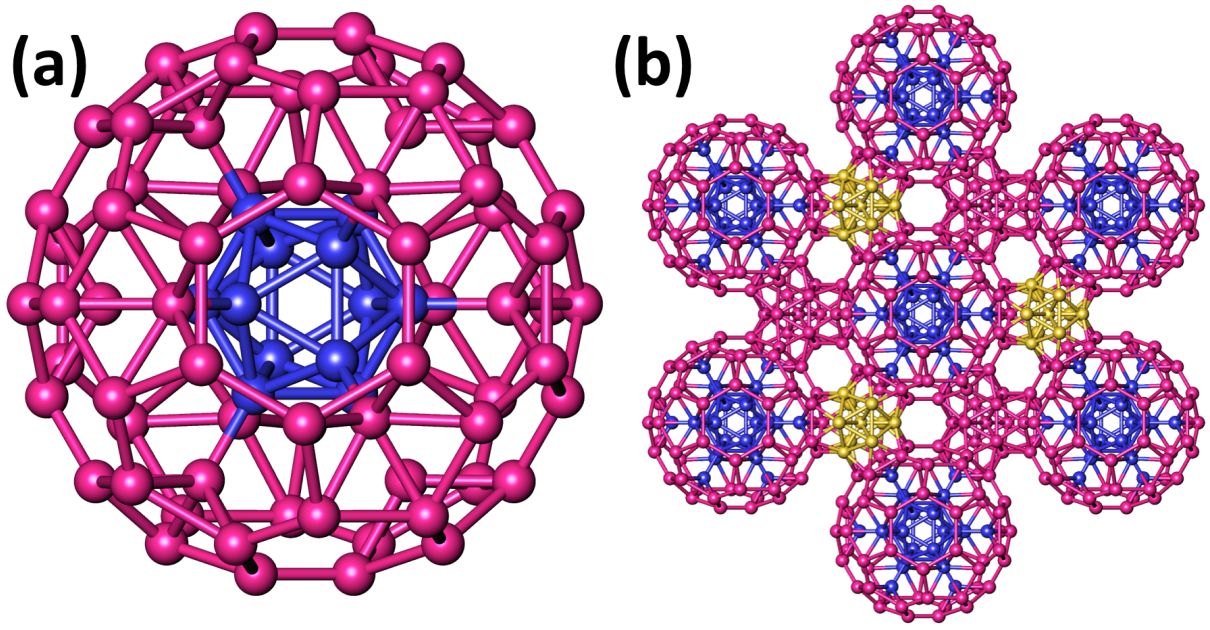

Figure 2. The crystal structure of β-rhombohedral boron in terms of B_{84} and B_{10} units. (a) B_{84} consists of a central B_{12} icosahedron (blue) surrounded by 12 half icosahedra (pink). (b) B_{84} units in adjacent rhombohedral unit cells connected via B_{10} cluster units (gold). This view is from the c-axis (perpendicular to the page). These layered structures stick to each other along this axis, and interstitial boron atoms (not drawn) lie between B_{10} clusters connecting the layers.

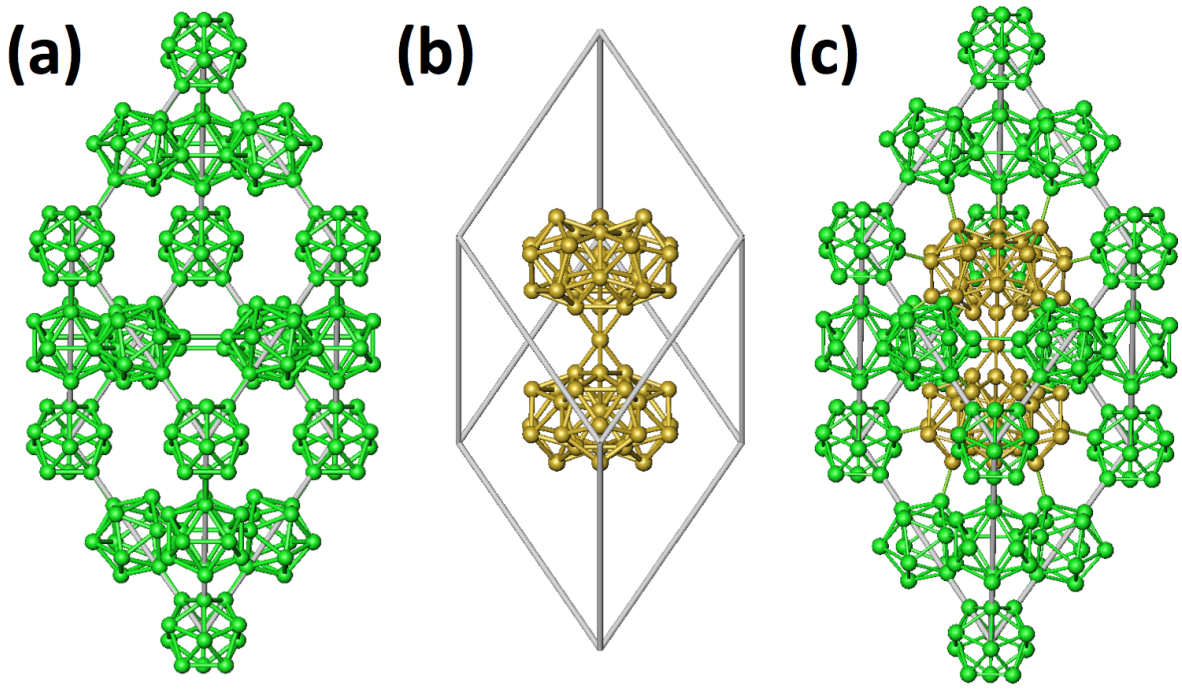

Figure 3. The crystal structure of β-rhombohedral boron in terms of B_{12} icosahedra (green) and B_{28} triply fused icosahedra (gold). The grey lines denote the rhombohedral unit cell. (a) Eight icosahedra (green) are located at the corners of the unit cell, and 12 icosahedra are located along the middle of each edge of the unit cell. (b) Two B_{28} triply fused icosahedra (gold) and the interstitial atom (gold) are located in the middle of the unit cell. (c) The icosahedra and the fused icosahedra are directly bonded to each other, with large holes between the different building units.

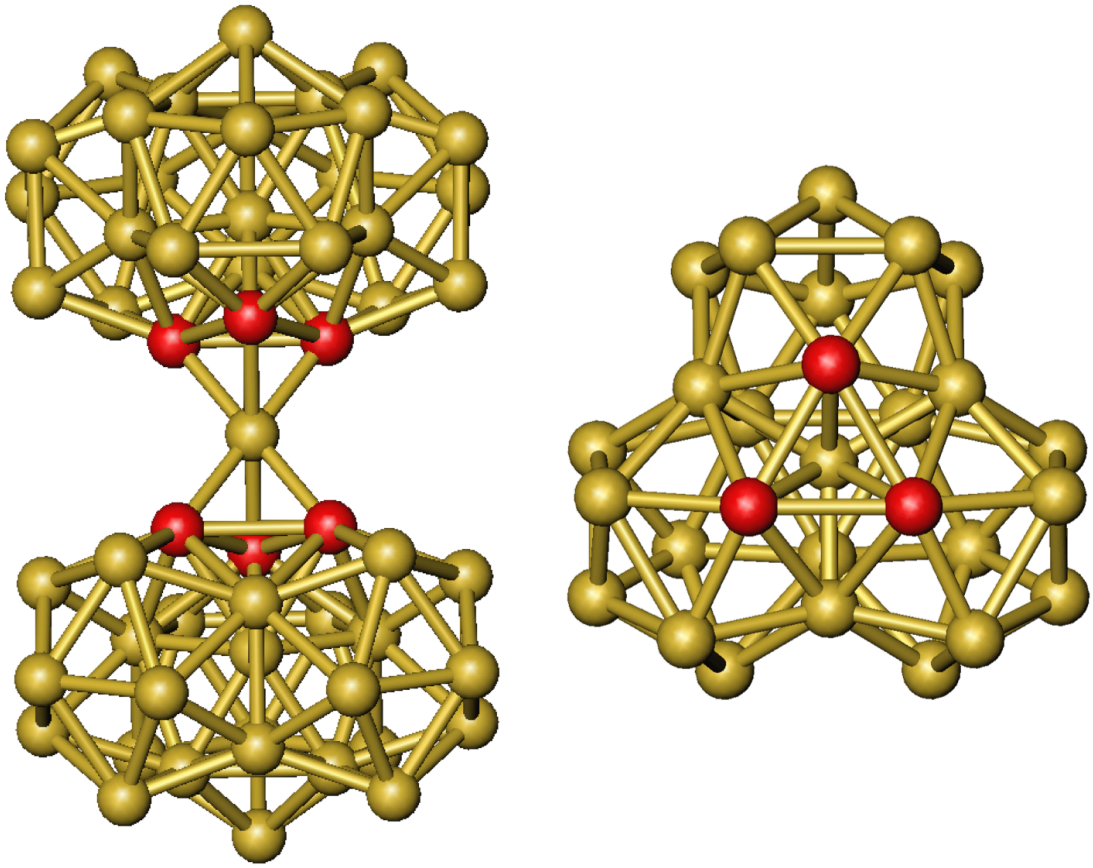

Figure 4. The B13 vacancy sites (red spheres) in a B_{28} cluster unit. Side view (left) and bottom view (right).

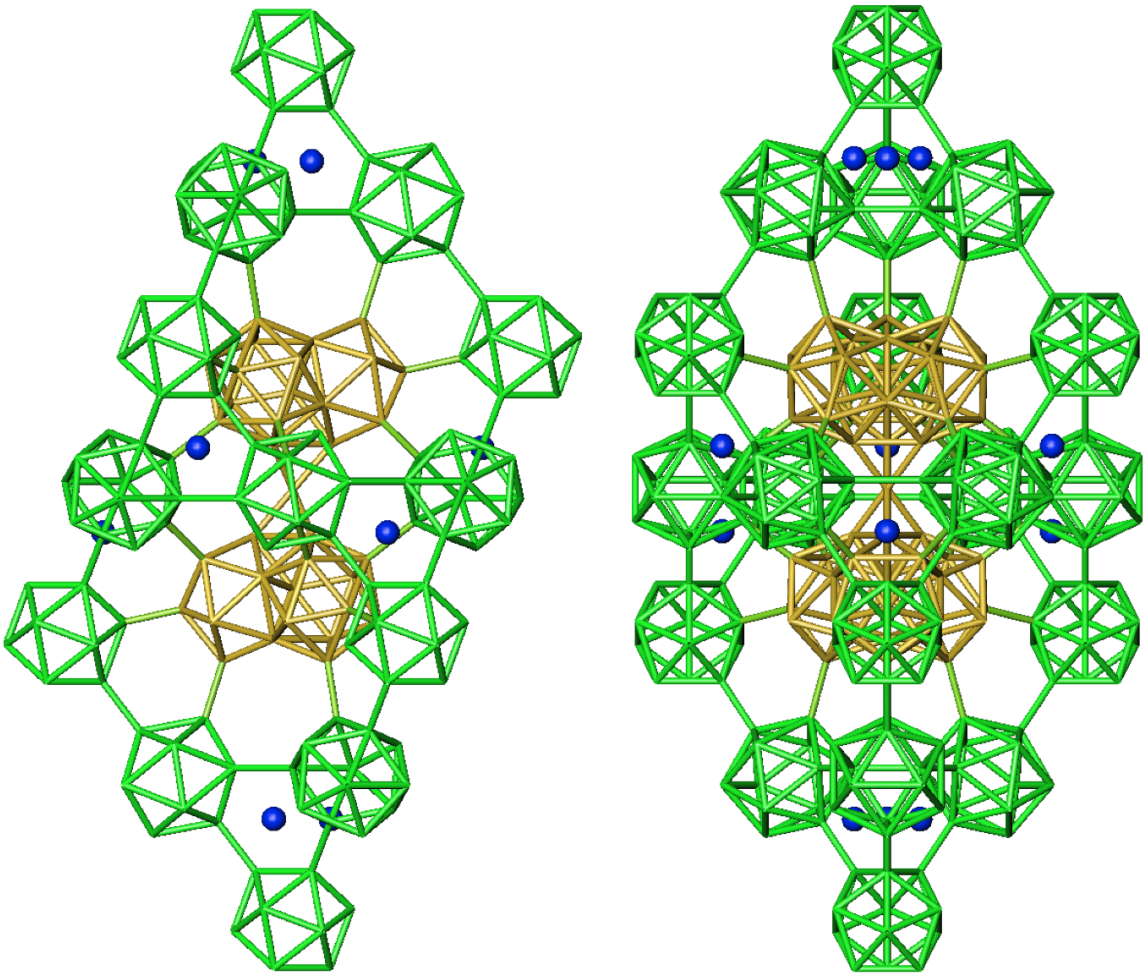

Figure 5. B16 interstitial POS (blue spheres) exist at the center of hexagonal rings connecting B_{12} icosahedra, as seen from different angles (left and right).

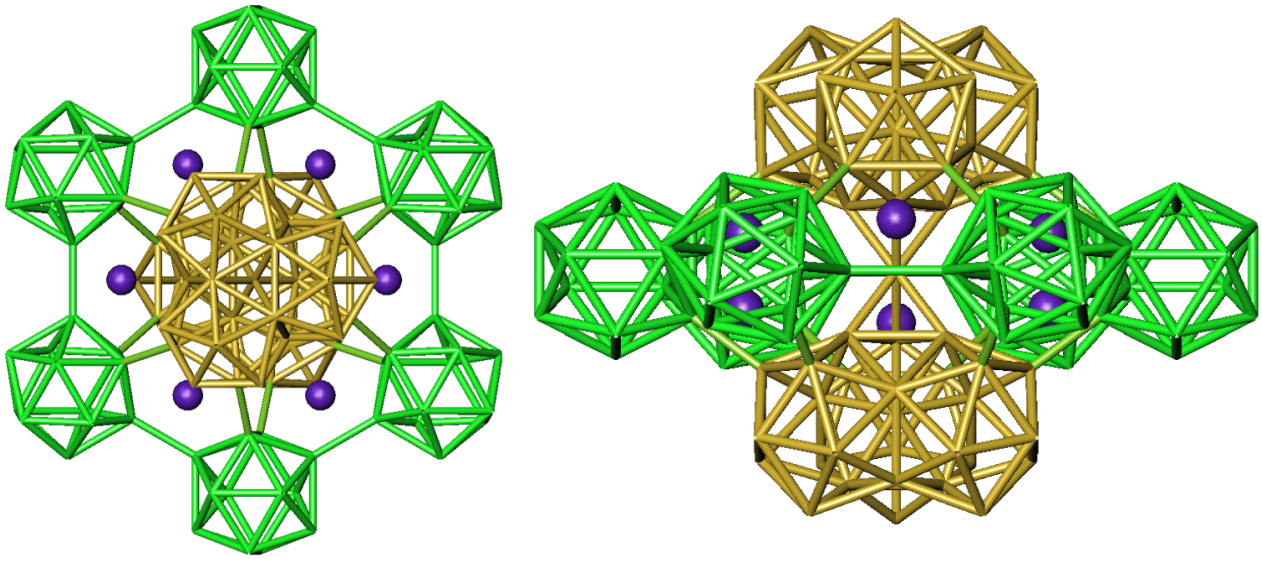

Figure 6. The B19 POS (purple spheres) are at the center of hexagonal rings connecting B_{12} icosahedra (green bonds) and B_{28} triply fused icosahedra (gold bonds), as seen from the top (left) and the side (right). Only the icosahedra at z=c/2 are drawn.

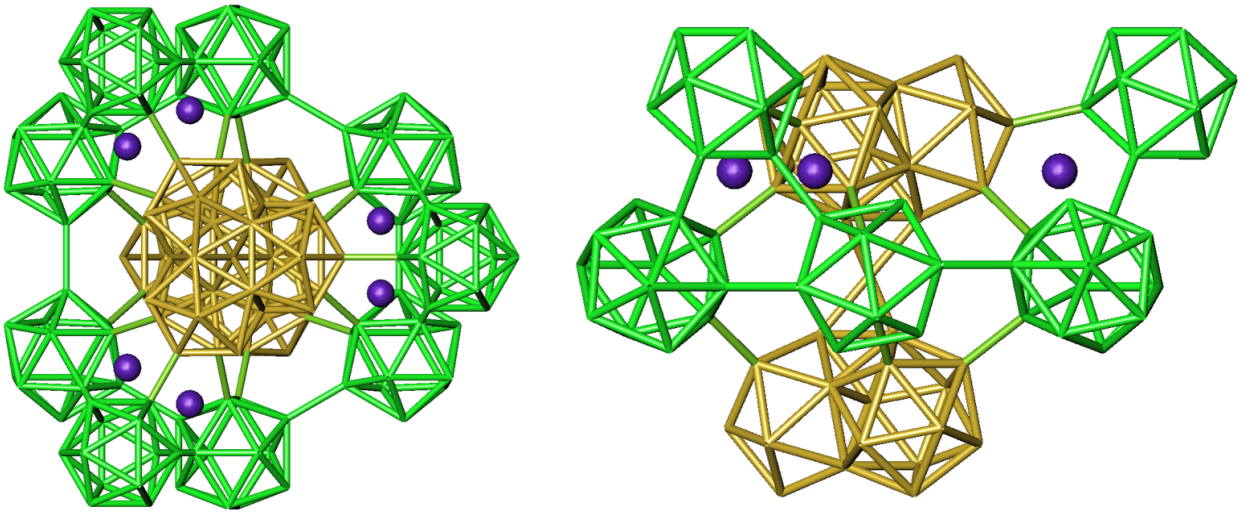

Figure 7. The locations of B20 POS (purple spheres) are at the center of hexagonal rings connecting the B_{12} icosahedra and B_{28} triply fused icosahedra, as seen from the top (left) and side (right). For the sake of clarity, only the upper half of B20s, and the associated B_{12} icosahedra are drawn.

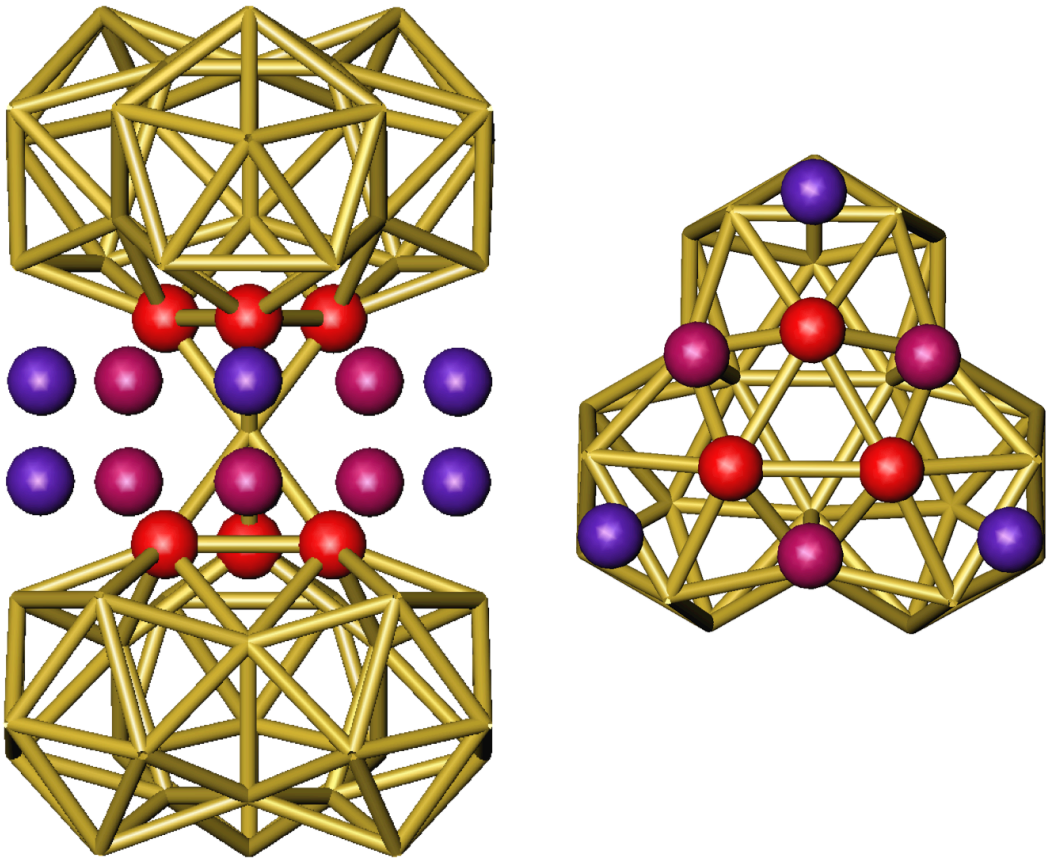

Figure 8. The B17 (magenta spheres) and B18 (purple spheres) POS surround the B13 vacancy (red spheres) sites, as seen from the side (left) and the bottom (right), with only the upper half drawn in the latter view.

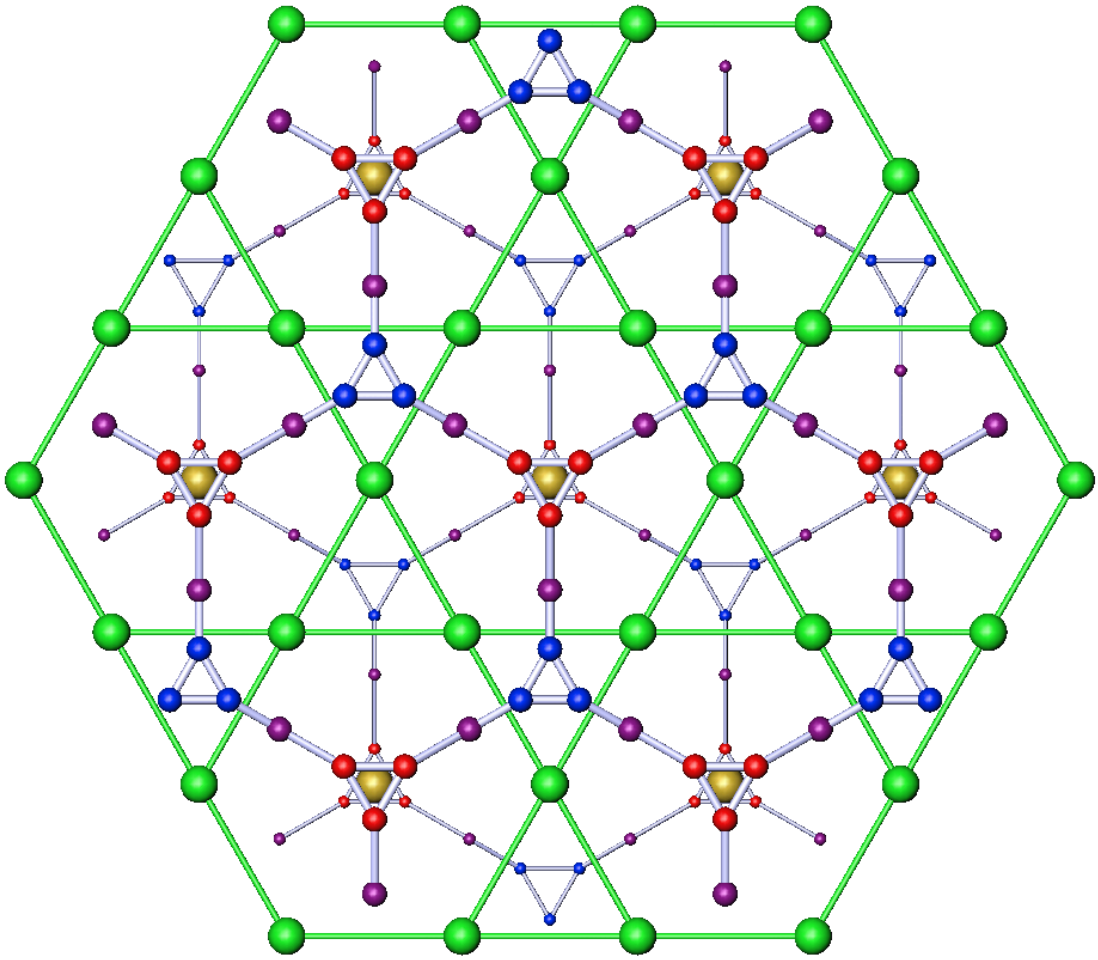

Figure 9. The kagome network of icosahedra (green spheres) and the two-dimensional POS network create a double layer–expanded kagome lattice. For clarity, only B13 (red), B16 (blue), and B19 (purple) POS are shown. The gold spheres are placed at the location of interstitial atoms connecting two triply fused icosahedra. Half of a POS network is depicted on the far side (thin bonds and small spheres), and the rest is on the near side (thick bonds and larger spheres) relative to the kagome network of icosahedra.

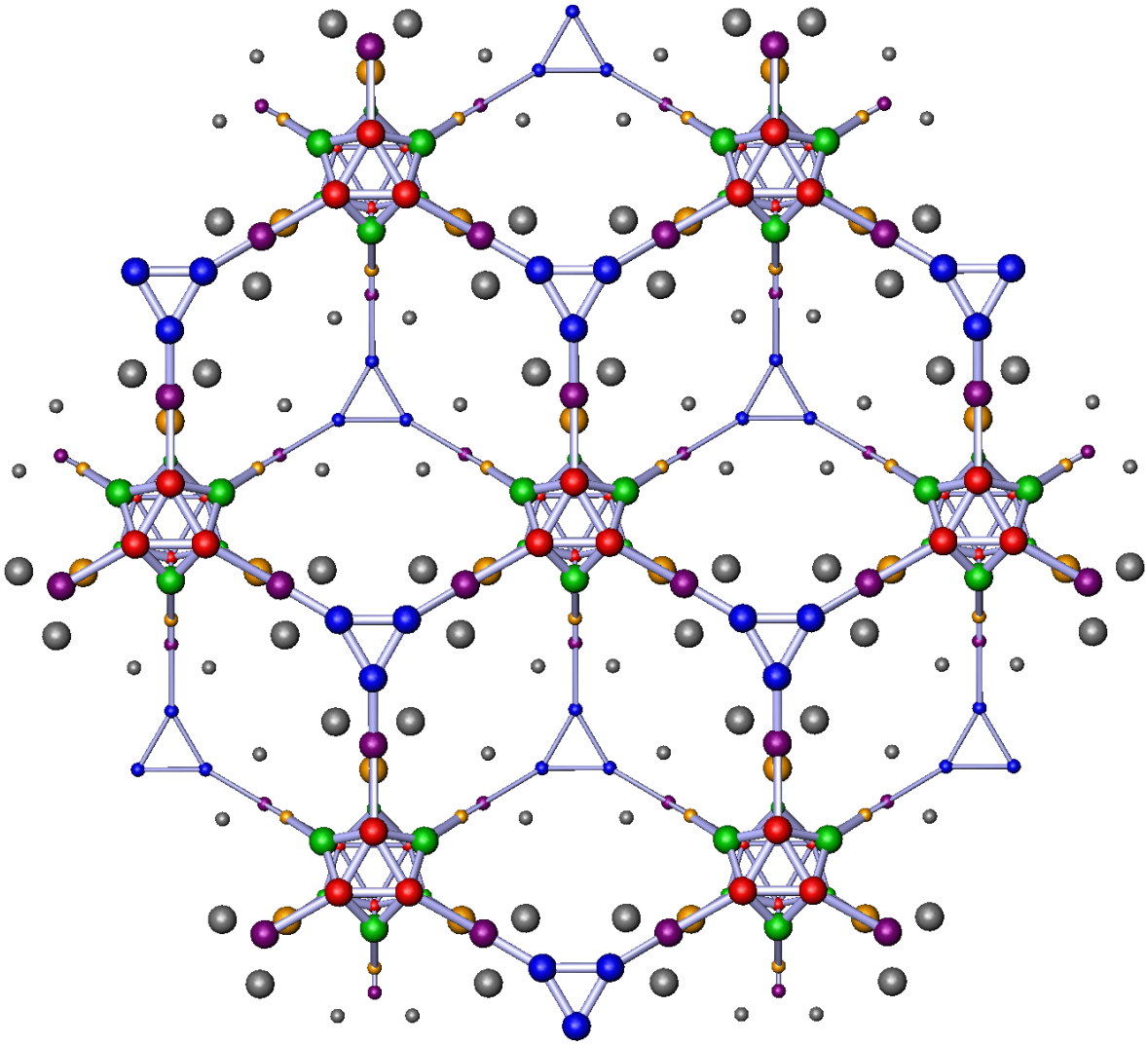

Figure 10. The location of POS in the double layer–expanded kagome lattice. B13 (red), B16 (blue), B17 (green), B18 (orange), B19 (purple), and B20 (grey). The thinner bonds and the smaller spheres are on the far side, and the thicker bonds and the large spheres are on the near side.

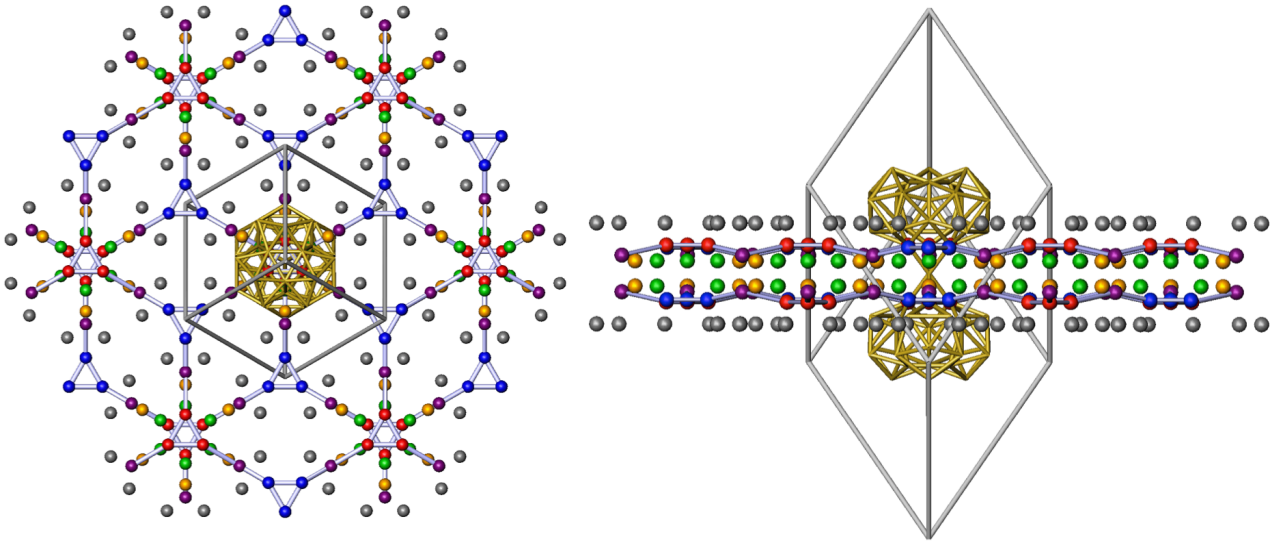

Figure 11. The quasi two-dimensional network of POS, $(2B_{28})B$, an inverted pair of triply fused icosahedra (gold bonds), and the rhombohedral unit-cell, as seen from the top (left) and side (right).

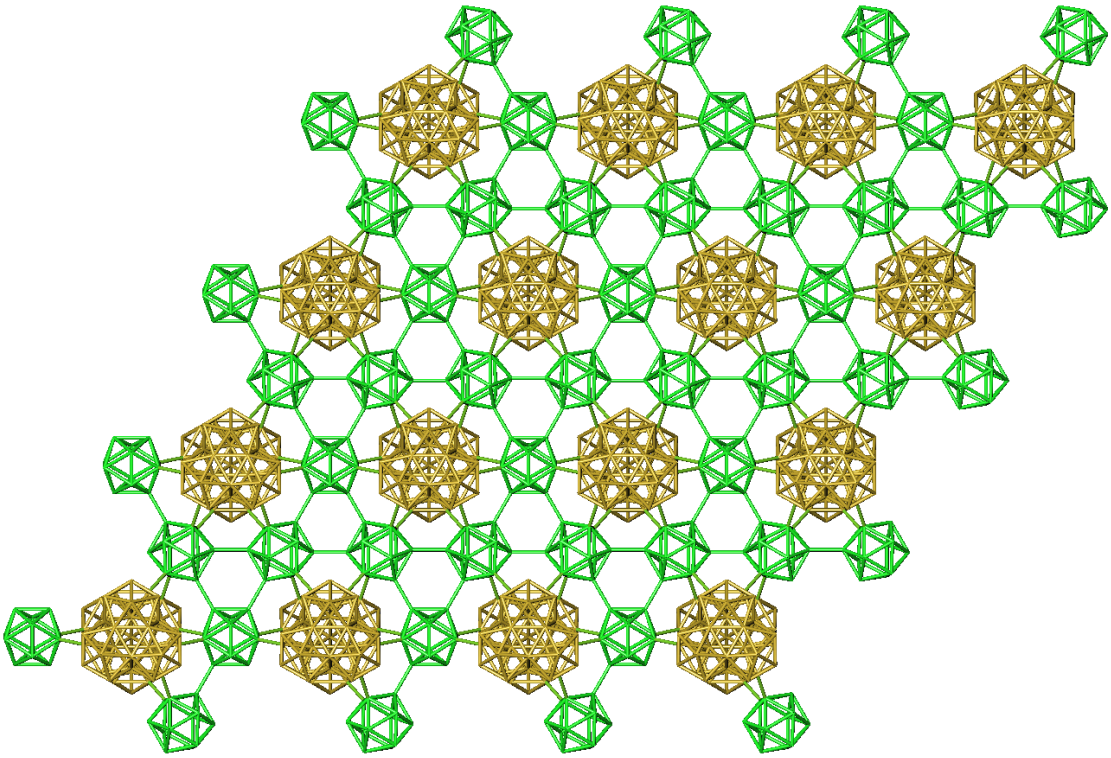

Figure 12. Kagome network of icosahedra at z=c/2 in β-boron (green bonds). The holes in the kagome network are occupied by an inverted pair of triply fused icosahedra (gold bonds).

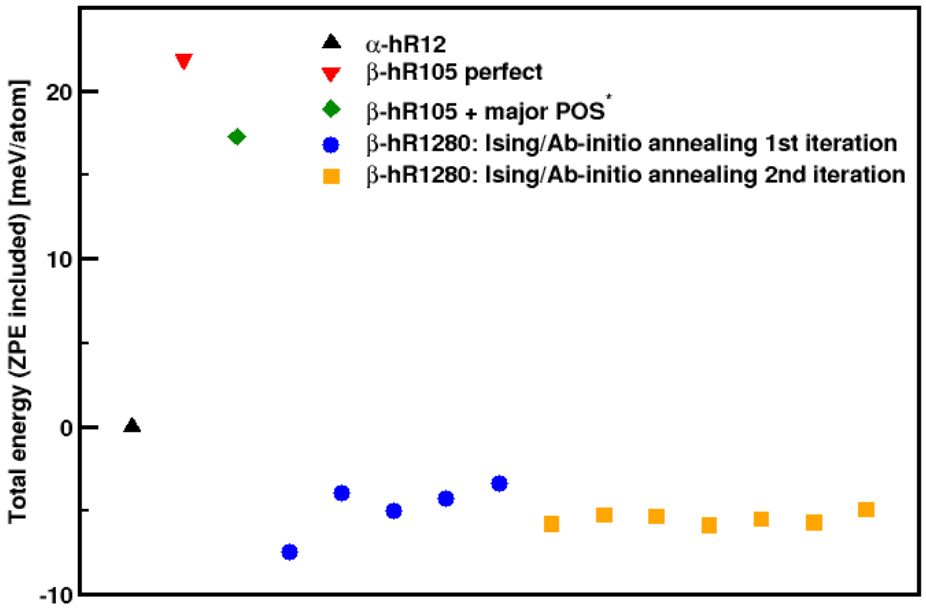

Figure 13. Relative *ab initio* DFT total energies, including the zero-point energy contribution, of α-rhombohedral boron (black triangle), perfect β-rhombohedral boron (red triangle, 105 atoms in the rhombohedral unit cell), and β-rhombohedral boron with only B13 and B16 POS[15] (green diamond). Blue circles and yellow squares are the *ab initio* DFT total energies of the hR1280 systems.[3k]

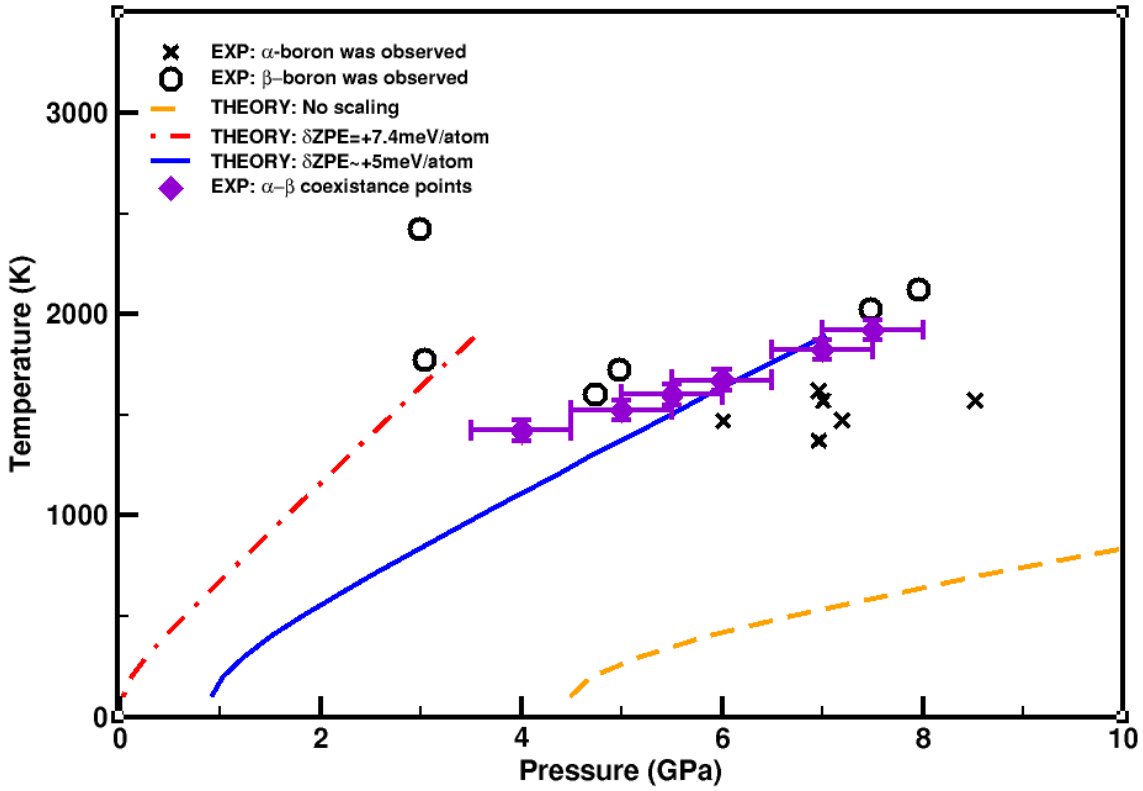

Figure 14. The α–β phase lines (THEORY) reported in Ref. 56 and recent high-pressure experimental measurements (EXP).[55] The experiments were conducted at the *P,T* points represented by the symbols:[55] α-boron was found to be stable at the crossings. β-boron was found to be stable at the open circles. The filled diamonds represent the inferred experimental α–β coexistence line. The lines correspond to theoretical α–β phase boundaries.[56] The dashed line was obtained without a scaling correction to the PDOS of β-boron. The dashed-dot line was obtained with the maximum scaling correction so that the α–β phase line intersects P=0 GPa at T=0 K. The solid line was obtained by applying a scaling correction that corresponds to an increase in the ZPE of β-boron of approximately +5 meV/atom. The γ-phase and T-phase are omitted from this plot for clarity.

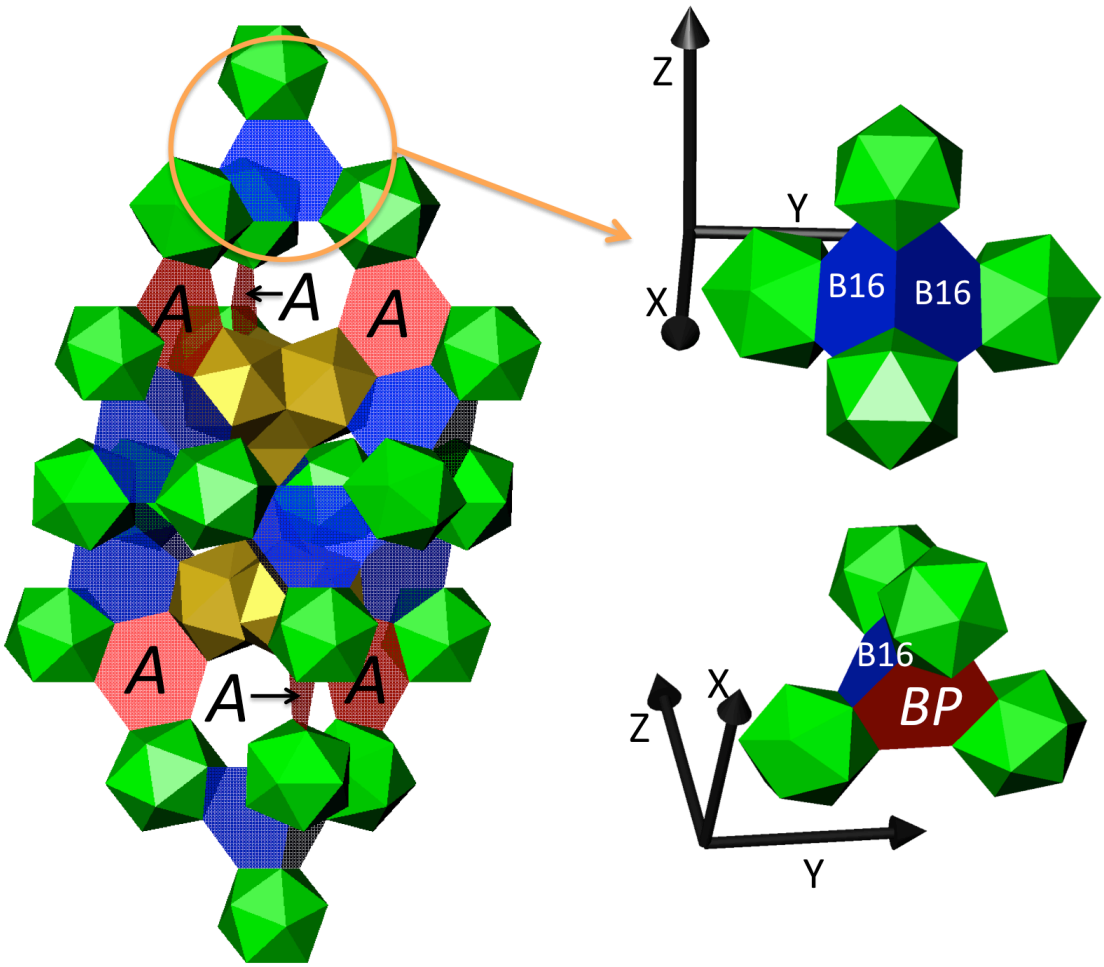

Figure 15. B_{12}s (green) and B_{28}s (gold) icosahedra are connected by hexagonal rings (red and blue), which can exhibit perfect self-doping by converting 2c2e bonds into 3c2e bonds. Only the blue hexagons are POS; the red ones are not occupied at all.

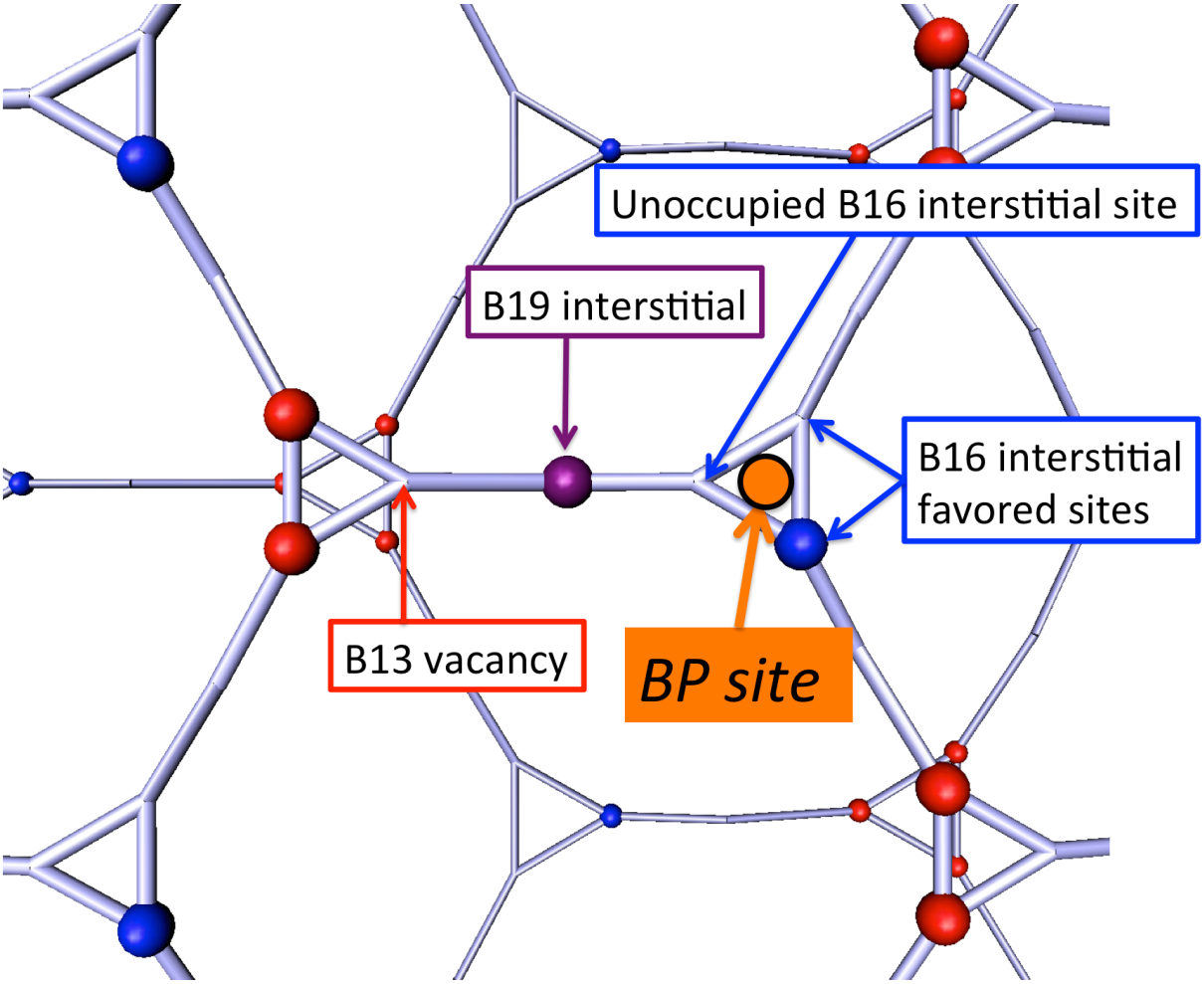

Figure 16. One of the ground state–POS configurations obtained in *ab initio* calculations, where the AF correlation between the sites B13, B19, and B16 can be seen. Site *BP*, which is not a POS, is located at the center of a B16 triangle (slightly off the plane). The distance between the B19 interstitial and the B16 (or *BP*) sites is the longest for favored sites and the shortest for unoccupied sites, consistent with the AF (repulsive) interaction between B19 and B16 (*BP*) sites.

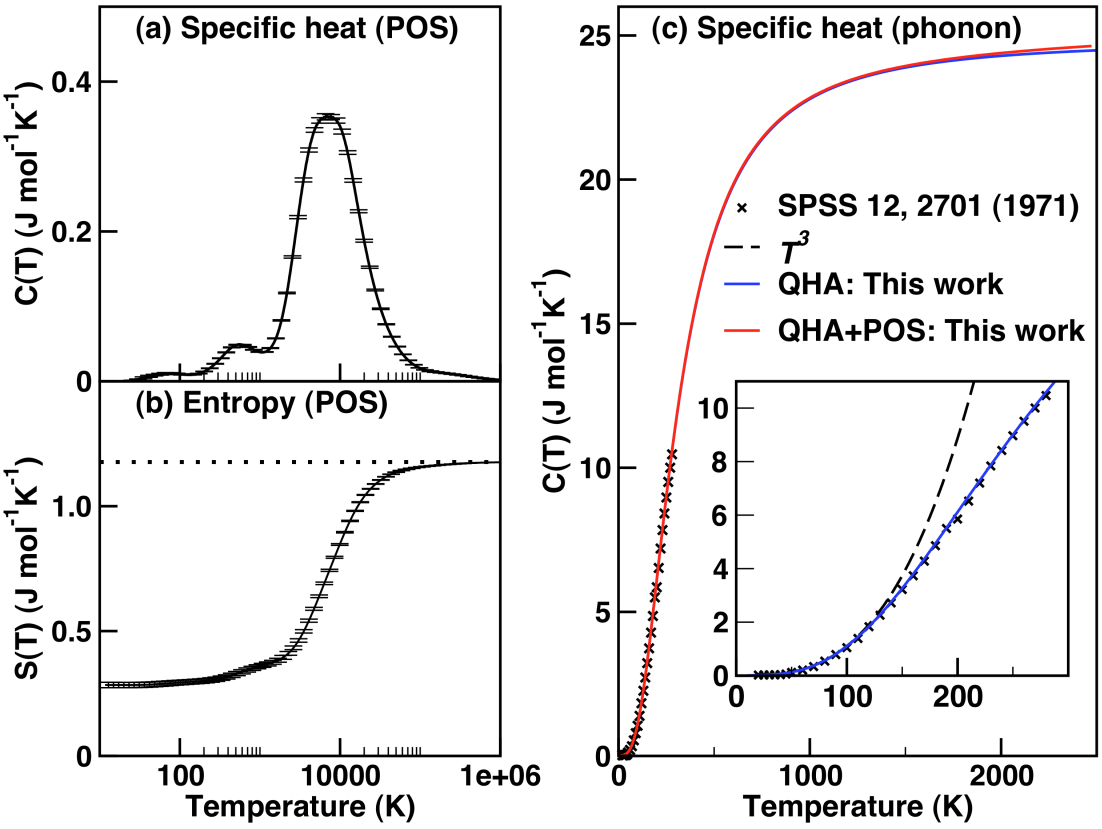

Figure 17. The configurational specific heat (a) and the entropy (b) of the POS. The theoretical total specific heat—the sum of phonon and configurational specific heat—and experimental values (c).[31]

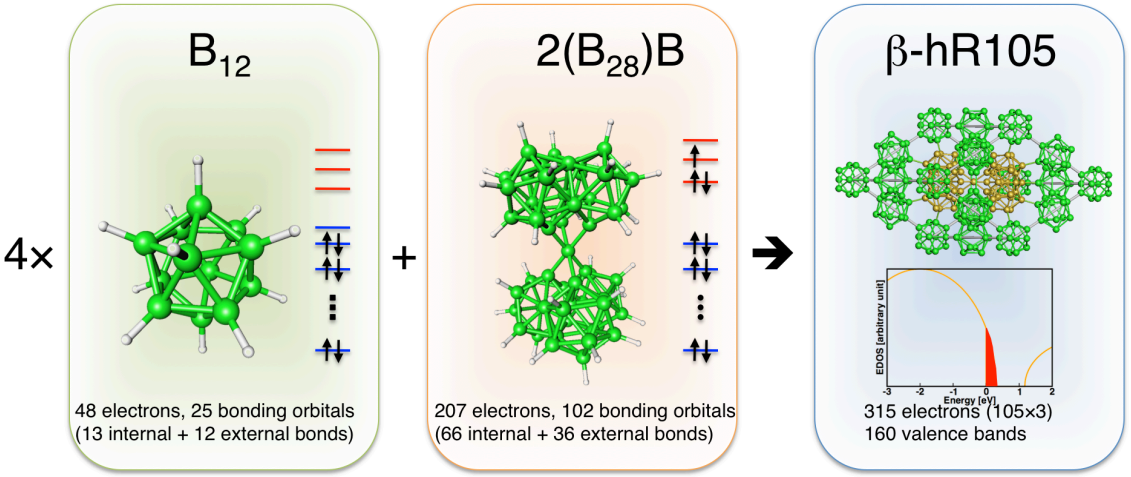

Electron count of β-hR105

Internal bonding orbitals

13×4 + 66 = 118

External bonding orbitals:

(12×4 + 36)/2 = 42

Total number of bonds:

118+42=160

(320 electrons)

105×3=315; 5 electrons short for the complete formation of bonds in β-hR105

Figure 18. Schematic diagrams of the electron requirements of building units B_{12} (left), $2(B_{28})B$ (center), and the solid phase β-hR105 (right) without POS; the diagrams illustrate how the total electron requirement of 320 electrons per unit cell can be described by units of B_{12} and $2(B_{28})B$.

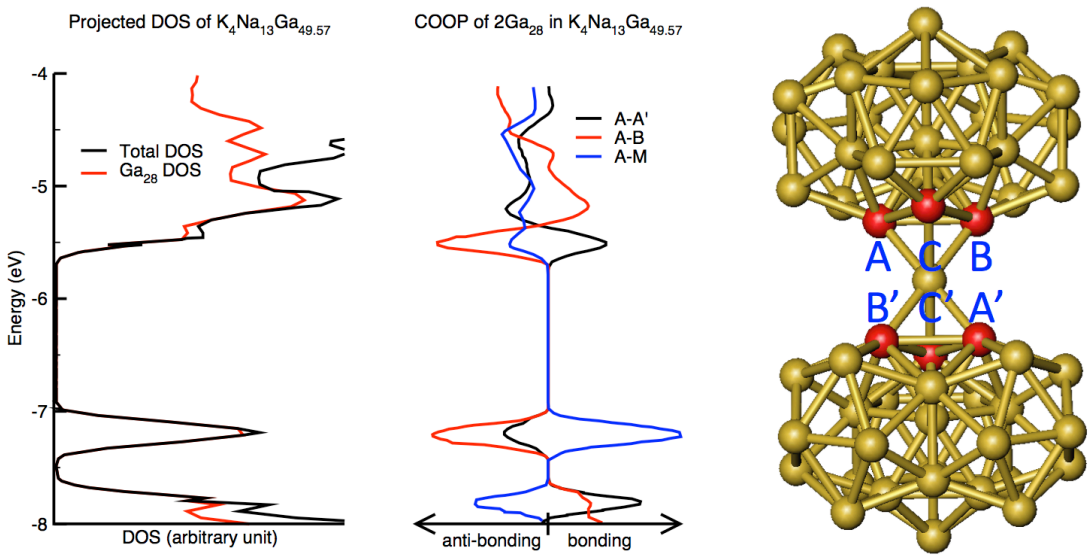

Figure 19. Density of states (DOS), projected DOS and crystal orbital overlap population (COOP) of the Ga_{28} cluster that appear in the Zintl phase – intermetallic compound $K_4Na_{13}Ga_{49.57}$.[14a] The Ga_{28} DOS (left) dominates the contribution to the total DOS near the Fermi level. The COOP analysis (middle) shows that the observed vacancies at A, B, and C (or A', B', and C') (right) are due to local anti-bonding orbitals and to the excess number of bonding electrons of Ga_{28}.[14a]

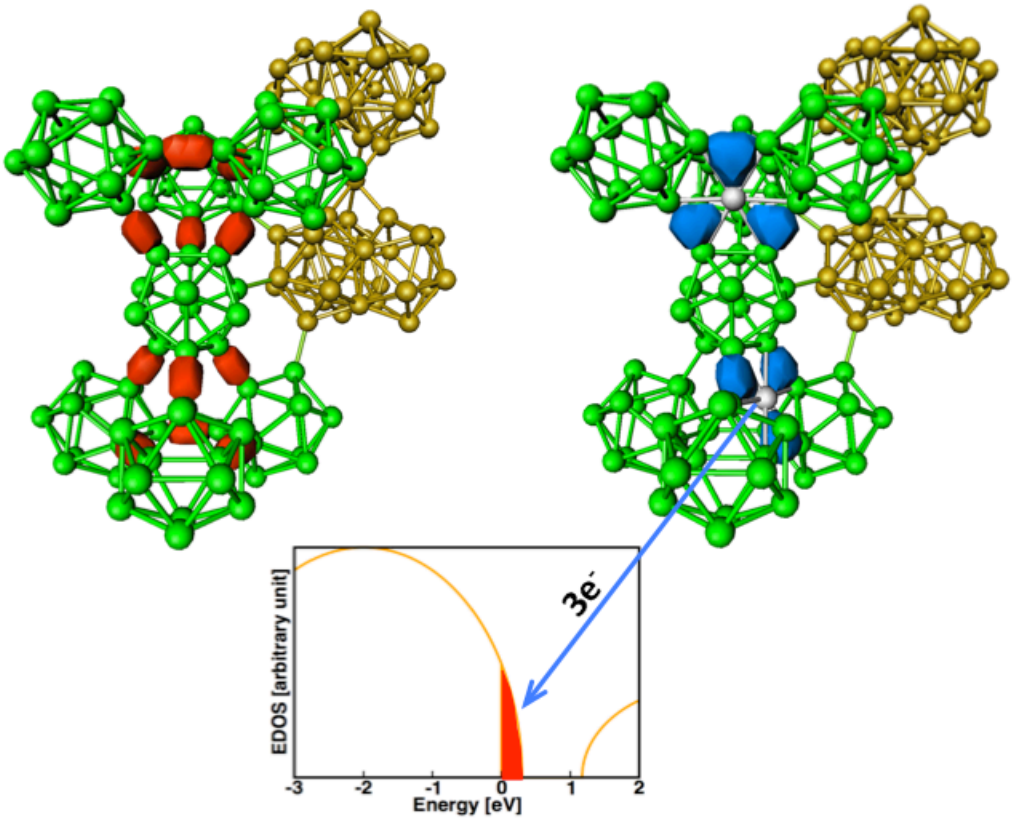

Figure 20. A schematic illustration describing how the occupation of B16 interstitials (grey spheres, upper right) self-dope β-rhombohedral boron, as described by Maximally Localized Wannier Functions (MLWFs).[3k] The hole states in the valence band of β-boron (red area in the plot of electronic density of states, middle) correspond to the inter-B_{12} 2c2e bonding (red isosurfaces, upper left). Upon occupation of a B16 site, three 2c2e bonds (red isosurfaces) are converted to three 3c2e bonds (blue isosurfaces). Each B16 interstitial supplies three valence electrons without changing the number of valence bands (or bonding states).

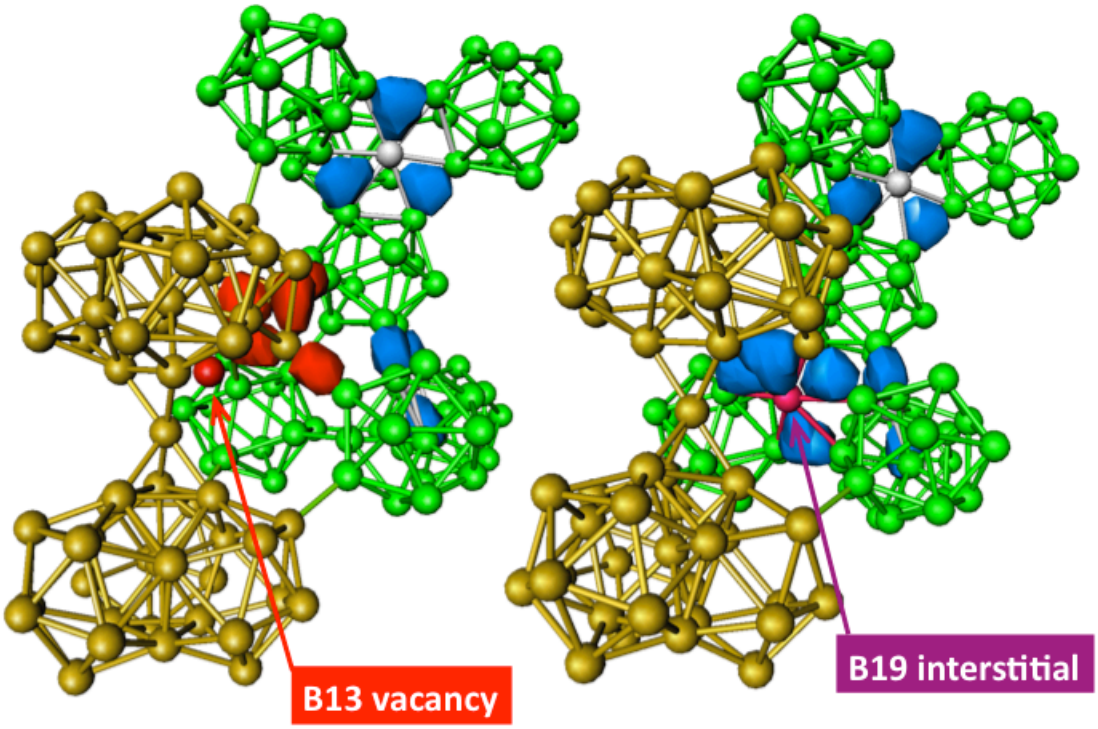

Figure 21. The stabilization mechanism due to the formation of the B13 vacancy and the B19 interstitial pair is described using MLWFs.[3k] A B13 vacancy is favored due to the local anti-bonding character of the orbitals (see Figure 13); dangling bonds (red isosurfaces) surround the B13 vacancy (left). Occupation of the B19 interstitial site that is closest to the B13 vacancy stabilizes the system by saturating the dangling bonds and by converting three 2c2e bonds to three 3c2e bonds (blue isosurfaces surrounding the B19 interstitial, right). In this case, the B19 occupation adds three valence electrons without changing the number of valence states (or bonding states). The energy gain due to such a vacancy-interstitial pair, in the language of spin magnetism, corresponds to an anti-ferromagnetic interaction between B13 and B19 sites.

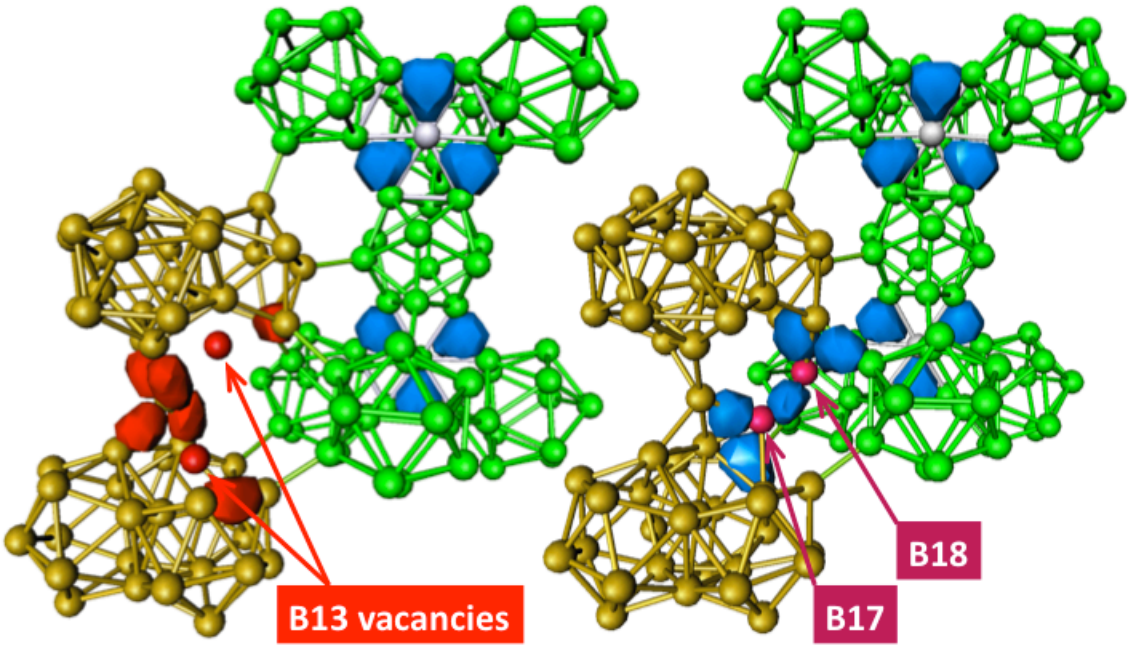

Figure 22. The stabilization mechanism due to the formation of a complex B13 vacancy pair and a B17-B18 interstitial pair is described using MLWFs.[3k] Two B13 vacancy pairs (two red spheres, left) in the opposing B_{28} units may be introduced to stabilize the $(2B_{28})B$ unit (see Figure 13), but at the expense of introducing dangling bonds (red isosurfaces, left). These dangling-bond states can be completely saturated by the introduction of a B17-B18 interstitial pair (purple spheres, right), leading to the introduction of an additional bonding state. In this case, no clear formation of 3c2e bonds is observed. This stabilization mechanism does not provide perfect self-doping and leaves hole states in the valence band at the experimental atomic density of 320 atoms per hexagonal cell.

(1) (a) Donohue, J. In *THE STRUCTURES OF THE ELEMENTS*; JOHN WILLEY & SONS: New York, London, Sydney, Toronto, 1974(b) Young, D. A. *Phase Diagrams of the Elements*; University of California Press: Berkeley Los Angeles Oxford, 1991(c) Chase, M. W. *Journal of Physical Chemistry Reference Data* **1998**, *9*(d) Douglas, B. *Structure and Chemistry of Crystalline Solid*; Springer Science + Business Media, Inc, 2006.

(2) Oganov, A. R.; Chen, J. H.; Gatti, C.; Ma, Y. Z.; Ma, Y. M.; Glass, C. W.; Liu, Z. X.; Yu, T.; Kurakevych, O. O.; Solozhenko, V. L. *Nature* **2009**, *457*, 863.

(3) (a) Sands, D. E.; Hoard, J. L. *Journal of the American Chemical Society* **1957**, *79*, 5582(b) Hoard, J. L.; Newkirk, A. E. *Journal of the American Chemical Society* **1960**, *82*, 70(c) Masago, A.; Shirai, K.; Katayama-Yoshida, H. In *Physics of Semiconductors, Pts A and B*; Menendez, J., VanDeWalle, C. G., Eds., 2005; Vol. 772(d) Prasad, D.; Balakrishnarajan, M. M.; Jemmis, E. D. *Physical Review B* **2005**, *72*, 195102(e) Masago, A.; Shirai, K.; Katayama-Yoshida, H. *Physical Review B* **2006**, *73*, 104102(f) van Setten, M. J.; Uijttewaal, M. A.; de Wijs, G. A.; de Groot, R. A. *Journal of the American Chemical Society* **2007**, *129*, 2458(g) Shirai, K.; Masago, A.; Katayama-Yoshida, H. *Physica Status Solidi B-Basic Solid State Physics* **2007**, *244*, 303(h) Shang, S. L.; Wang, Y.; Arroyave, R.; Liu, Z. K. *Physical Review B* **2007**, *75*, 092101(i) Widom, M.; Mihalkovic, M. *Physical Review B* **2008**, *77*, 064113(j) Widom, M.; Mihalkovic, M. In *16th International Symposium on Boron, Borides and Related Materials*; Tanaka, T., Ed., 2009; Vol. 176(k) Ogitsu, T.; Gygi, F.; Reed, J.; Motome, Y.; Schwegler, E.; Galli, G. *Journal of the American Chemical Society* **2009**, *131*, 1903(l) Ogitsu, T.; Gygi, F.; Reed, J.; Udagawa, M.; Motome, Y.; Schwegler, E.; Galli, G. *Physical Review B* **2010**, *81*, 020102.

(4) (a) Hoard, J. L.; Geller, S.; Hughes, R. E. *Journal of the American Chemical Society* **1951**, *73*, 1892(b) Longuet-Higgins, H. C.; Roberts, M. D. *Proceedings of the Royal Society of London Series a-Mathematical and Physical Sciences* **1955**, *230*, 110(c) Hoard, J. L.; Hughes, R. E.; Sands, D. E. *Journal of the American Chemical Society* **1958**, *80*, 4507(d) Amberger, E.; Ploog, K. *Journal of the Less-Common Metals* **1968**, *15*, 240(e) Ploog, K.; Kossobut.Kh; Amberger, E.; Schmidt, H.; Will, G. *Journal of the Less-Common Metals* **1972**, *29*, 161(f) Will, G.; Ploog, K. *Nature* **1974**, *251*, 406(g) Vlasse, M.; Naslain, R.; Kasper, J. S.; Ploog, K. *Journal of Solid State Chemistry* **1979**, *28*, 289(h) Bylander, D. M.; Kleinman, L.; Lee, S. *Physical Review B* **1990**, *42*, 1394(i) Bylander, D. M.; Kleinman, L. *Physical Review B* **1991**, *43*, 1487(j) Lee, S.; Bylander, D. M.; Kim, S. W.; Kleinman, L. *Physical Review B* **1992**, *45*, 3248(k) Li, D.; Xu, Y. N.; Ching, W. Y. *Physical Review B* **1992**, *45*, 5895(l) Kurakevych, O. O.; Le Godec, Y.; Hammouda, T.; Goujon, C. *High Pressure Research* **2011**, *32*, 30(m) Evgeny, A. E.; Igor, P. Z. *Science and Technology of Advanced Materials* **2011**, *12*, 055009(n) Qin, J. Q.; Irifune, T.; Dekura, H.; Ohfuji, H.; Nishiyama, N.; Lei, L.; Shinmei, T. *Physical Review B* **2012**, *85*, 014107.

(5) (a) Horn, F. H. *Journal of Applied Physics* **1959**, *30*, 1612(b) Tavadze, F. N.; Bairamas.Ia; Tsagarei.Gv; Tsomaya, K. P.; Zoidze, N. A. *Soviet Physics Crystallography, Ussr* **1965**, *9*, 768.

(6) Hughes, R. E.; Sullenge.Db; Weakliem, H. A.; Kennard, C. H. L.; Sands, D. E.; Hoard, J. L. *Journal of the American Chemical Society* **1963**, *85*, 361.

(7) (a) Runow, P. *Journal of Materials Science* **1972**, *7*, 499(b) Carlsson, J. O. *Journal of the Less-Common Metals* **1980**, *70*, 77.

(8) (a) J. L. Hoard, D. B. S., C. H. L. Kennard, and R. E. Hughes *Journal of Solid State Chemistry* **1970**, *1*, 268(b) Bullett, D. W. *Journal of Physics C-Solid State Physics* **1982**, *15*, 415(c) Slack, G. A.; Hejna, C. I.; Garbauskas, M. F.; Kasper, J. S. *Journal of Solid State Chemistry* **1988**, *76*, 52.
(9) Szadkowski, A. *Journal of the Less-Common Metals* **1979**, *67*, 551.
(10) (a) Werheit, H.; Laux, M.; Kuhlmann, U. *Physica Status Solidi B-Basic Research* **1993**, *176*, 415(b) Golikova, O. A. *Physica Status Solidi a-Applied Research* **1979**, *51*, 11.
(11) (a) Everhardt, W. H.; Crawford Jr, B.; Lipscomb, W. N. *The Journal of Chemical Physics* **1954**, *22*, 989(b) Durant, P. J.; Durant, B. In *INTRODUCTION TO ADVANCED INORGANIC CHEMISTRY*; SECOND ed.; JOHN WILEY & SONS, INC: New York, 1970(c) Longuet-Higgins, H. C.; Bell, R. P. *Journal of the Chemical Society* **1943**, 250.
(12) Pitochelli, A. R.; Hawthorne, M. F. *Journal of the American Chemical Society* **1960**, *82*, 3228.
(13) (a) Jemmis, E. D.; Balakrishnarajan, M. M. *Journal of the American Chemical Society* **2001**, *123*, 4324(b) Jemmis, E. D.; Prasad, D. *Journal of Solid State Chemistry* **2006**, *179*, 2768.
(14) (a) Tillard-Charbonnel, M.; Manteghetti, A.; Belin, C. *Inorganic Chemistry* **2000**, *39*, 1684(b) Balakrishnarajan, M. M.; Jemmis, E. D. *Journal of the American Chemical Society* **2000**, *122*, 4516.
(15) Masago, A.; Shirai, K.; Katayama-Yoshida, H. *Molecular Simulation* **2004**, *30*, 935.
(16) (a) Bernal, J. D.; Fowler, R. H. *Journal of Chemical Physics* **1933**, *1*, 515(b) Giauque, W. F.; Ashley, M. F. *Physical Review* **1933**, *43*, 81(c) Pauling, L. *Journal of the American Chemical Society* **1935**, *57*, 2680(d) Giauque, W. F.; Stout, J. W. *Journal of the American Chemical Society* **1936**, *58*, 1144(e) Lieb, E. H. *Physical Review* **1967**, *162*, 162(f) Lieb, E. H. *Physical Review Letters* **1967**, *18*, 692(g) Harris, M. J.; Bramwell, S. T.; McMorrow, D. F.; Zeiske, T.; Godfrey, K. W. *Physical Review Letters* **1997**, *79*, 2554(h) Bramwell, S. T.; Gingras, M. J. P. *Science* **2001**, *294*, 1495.
(17) Anderson, P. W. *Phys Rev* **1956**, *102*, 1008.
(18) (a) Tsagareishvili, G. V.; Tavadzf, F. N.; Darsavelidze, G. S.; Metreveli, V. S. Boron, Walsaw, Poland, 1968; p 281(b) Zareba, A.; Lubomirs.A *Physica Status Solidi* **1969**, *34*, K41(c) Young, J. D.; Oliver, D. W.; Slack, G. A. *Applied Physics Letters* **1969**, *14*, 301(d) Werheit, H. *Physica Status Solidi* **1970**, *39*, 109(e) Kubler, L.; Gewinner, G.; Koulmann, J. J.; Jaegle, A. *Physica Status Solidi B-Basic Research* **1973**, *60*, 117(f) Gewinner, G.; Kubler, L.; Koulmann, J. J.; Jaegle, A. *Physica Status Solidi B-Basic Research* **1973**, *59*, 395(g) Geist, D. *Zeitschrift Fur Naturforschung Section a-a Journal of Physical Sciences* **1973**, *28*, 953(h) Siems, C. D.; Geist, D. *Journal of the Less-Common Metals* **1976**, *47*, 79(i) Tavadze, F. N.; Khachapuridze, R. A.; Darsavelidze, G. S.; Tsagareishvili, G. V.; Tavadze, G. F. *Journal of the Less-Common Metals* **1979**, *67*, 269(j) Darsavelidze, G. S.; Tavadze, F. N.; Metreveli, V. S.; Tsagareishvili, O. A.; Khachapuridze, R. A.; Nikuradze, I. G. *Journal of the Less-Common Metals* **1981**, *82*, 361(k) Darsavelidze, G. S.; Tsagareishvili, G. V.; Tsirlin, M. A.; Nikuradze, J. G.; Tsagareishvili, O. A.; Zhigach, A. F.; Tavadze, F. N. *Journal of the Less-Common Metals* **1979**, *67*, 471(l) Werheit, H.; Franz, R. *Physica Status Solidi B-Basic Research* **1984**, *125*, 779(m) Werheit, H.; Franz, R. *Journal of the Less-Common Metals* **1986**, *117*, 163(n) Werheit, H.; Wehmoller, B. *Journal of Solid State Chemistry* **2004**, *177*, 556.

(19) (a) Mori, T. In *Handbook on the Physics and Chemistry of Rare Earths*; Gschneidner, K. A. J., Bunzli, J. C., Pecharsky, V., Eds.; Elsevier: Amsterdam, 2008(b) Albert, B.; Hillebrecht, H. *Angewandte Chemie-International Edition* **2009**, *48*, 8640.
(20) Oganov, A. R.; Solozhenko, V. L. *J Sup Mat* **2009**, *31*, 285.
(21) (a) Jemmis, E. D.; Balakrishnarajan, M. M.; Pancharatna, P. D. *Chemical Reviews* **2002**, *102*, 93(b) Jemmis, E. D.; Prasad, D. L. V. K. *Current Science* **2009**, *95*, 1277.
(22) Werheit, H. In *16th International Symposium on Boron, Borides and Related Materials*; Tanaka, T., Ed., 2009; Vol. 176.
(23) Shirai, K. *Journal of Superhard Materials* **2010**, *32*, 205.
(24) (a) Shimizu, K.; Kaneshige, M.; Hashimoto, Y.; Nagatochi, T.; Hyodo, H.; Kimura, K. *Physica C-Superconductivity and Its Applications* **2010**, *470*, S631(b) Shirai, K.; Dekura, H.; Mori, Y.; Fujii, Y.; Hyodo, H.; Kimura, K. *Journal of the Physical Society of Japan* **2011**, *80*, 084601(c) Parakhonskiy, G.; Dubrovinskaia, N.; Dubrovinsky, L.; Mondal, S.; van Smaalen, S. *Journal of Crystal Growth* **2011**, *321*, 162(d) Nagatochi, T.; Hyodo, H.; Sumiyoshi, A.; Soga, K.; Sato, Y.; Terauchi, M.; Esaka, F.; Kimura, K. *Physical Review B* **2011**, *83*, 184507(e) Dekura, H.; Shirai, K.; Yanase, A. *Physical Review B* **2011**, *84*, 094117.
(25) (a) Zarechnaya, E. Y.; Dubrovinskaia, N.; Dubrovinsky, L.; Filinchuk, Y.; Chernyshov, D.; Dmitriev, V. *Journal of Crystal Growth* **2010**, *312*, 3388(b) Zarechnaya, E.; Dubrovinskaia, N.; Caracas, R.; Merlini, M.; Hanfland, M.; Filinchuk, Y.; Chernyshov, D.; Dmitriev, V.; Dubrovinsky, L. *Physical Review B* **2010**, *82*, 184111(c) Werheit, H.; Filipov, V.; Kuhlmann, U.; Schwarz, U.; Armbruster, M.; Leithe-Jasper, A.; Tanaka, T.; Higashi, I.; Lundstrom, T.; Gurin, V. N.; Korsukova, M. M. *Science and Technology of Advanced Materials* **2010**, *11*, 012001(d) Shirai, K. *Journal of Superhard Materials* **2010**, *32*, 336(e) Oganov, A. R.; Ma, Y. M.; Lyakhov, A. O.; Valle, M.; Gatti, C. In *High-Pressure Crystallography: From Fundamental Phenomena to Technological Applications*; Boldyreva, E., Dera, P., Eds., 2010(f) Oganov, A. R. In *Boron Rich Solids: Sensors, Ultra High Temperature Ceramics, Thermoelectrics, Armor*; Orlovskaya, N., Lugovy, M., Eds., 2010(g) Haussermann, U.; Mikhaylushkin, A. S. *Inorganic Chemistry* **2010**, *49*, 11270(h) Dubrovinskaia, N.; Dubrovinsky, L. In *High-Pressure Crystallography: From Fundamental Phenomena to Technological Applications*; Boldyreva, E., Dera, P., Eds., 2010(i) Zhou, X. F.; Tian, Y.; Wang, H. T. *Journal of Superhard Materials* **2011**, *33*, 401(j) Rulis, P.; Wang, L.; Walker, B.; Ching, W. Y. *Journal of Superhard Materials* **2011**, *33*, 394(k) Oganov, A. R.; Solozhenko, V. L.; Gatti, C.; Kurakevych, O. O.; Le Godec, Y. *Journal of Superhard Materials* **2011**, *33*, 363(l) Mondal, S.; van Smaalen, S.; Sch; ouml; nleber, A.; Filinchuk, Y.; Chernyshov, D.; Simak, S. I.; Mikhaylushkin, A. S.; Abrikosov, I. A.; Zarechnaya, E.; Dubrovinsky, L.; Dubrovinskaia, N. *Phys Rev Lett* **2011**, *106*, 215502(m) Macchi, P. *Journal of Superhard Materials* **2011**, *33*, 380(n) Le Godec, Y. *Journal of Superhard Materials* **2011**, *33*, 388(o) Kurakevych, O. O.; Solozhenko, V. L. *High Pressure Research* **2011**, *31*, 48(p) Isaev, E. I.; Simak, S. I.; Mikhaylushkin, A. S.; Vekilov, Y. K.; Zarechnaya, E. Y.; Dubrovinsky, L.; Dubrovinskaia, N.; Merlini, M.; Hanfland, M.; Abrikosov, I. A. *Physical Review B* **2011**, *83*, 132106(q) Aydin, S.; Simsek, M. *Journal of Alloys and Compounds* **2011**, *509*, 5219.

(26) (a) McCarty, L. V.; Kasper, J. S.; Horn, F. H.; Decker, B. F.; Newkirk, A. E. *Journal of the American Chemical Society* **1958**, *80*, 2592(b) Decker, B. F.; Kasper, J. S. *Acta Crystallographica* **1959**, *12*, 503.
(27) (a) Talley, C. P. *Acta Crystallographica* **1960**, *13*, 271(b) Vlasse, M.; Naslain, R.; Kasper, J. S.; Ploog, K. *Journal of the Less-Common Metals* **1979**, *67*, 1(c) Burdett, J. K.; Canadell, E. *Inorganic Chemistry* **1991**, *30*, 1991.
(28) (a) Zarechnaya, E. Y.; Dubrovinsky, L.; Dubrovinskaia, N.; Miyajima, N.; Filinchuk, Y.; Chernyshov, D.; Dmitriev, V. *Science and Technology of Advanced Materials* **2008**, *9*, 044209(b) Zarechnaya, E. Y.; Dubrovinsky, L.; Dubrovinskaia, N.; Filinchuk, Y.; Chernyshov, D.; Dmitriev, V.; Miyajima, N.; El Goresy, A.; Braun, H. F.; Van Smaalen, S.; Kantor, I.; Kantor, A.; Prakapenka, V.; Hanfland, M.; Mikhaylushkin, A. S.; Abrikosov, I. A.; Simak, S. I. *Physical Review Letters* **2009**, *102*, 185501(c) Oganov, A. R.; Chen, J. H.; Gatti, C.; Ma, Y. Z.; Ma, Y. M.; Glass, C. W.; Liu, Z. X.; Yu, T.; Kurakevych, O. O.; Solozhenko, V. L. *Nature* **2009**, *460*, 292.
(29) Weintraub, E. *Trans. Amer. Electrochem. Soc.* **1909**, *16*, 165.
(30) (a) Hackspill, L. *Comptes Rendus Hebdomadaires Des Seances De L Academie Des Sciences* **1931**, *193*, 776(b) Hackspill, L. *Helvetica Chimica Acta* **1933**, *16*, 1099.
(31) (a) Laugbengayer, A. W.; Newkirk, A. E.; Brandaur, R. L. *Journal of Chemical Education* **1942**, *19*, 382(b) Winslow, E. H.; Liebhafsky, H. A. *Journal of the American Chemical Society* **1942**, *64*, 2725(c) Laubengayer, A. W.; Hurd, D. T.; Newkirk, A. E.; Hoard, J. L. *Journal of the American Chemical Society* **1943**, *65*, 1924.
(32) (a) Will, G.; Kossobutzki, K. H. *Zeitschrift Fur Kristallographie* **1975**, *142*, 384(b) Will, G.; Kossobutzki, K. H. *Journal of the Less-Common Metals* **1976**, *47*, 33.
(33) Threlfall, T. *Organic Process Research & Development* **2003**, *7*, 1017.
(34) Kolakowski, B. *Acta Phsica Polonica* **1962**, *22*, 339.
(35) Geist, D.; Kloss, R.; Follner, H. *Acta Crystallographica Section B-Structural Crystallography and Crystal Chemistry* **1970**, *B 26*, 1800.
(36) Callmer, B. *Acta Crystallographica Section B-Structural Science* **1977**, *33*, 1951.
(37) Perrot, F. *Physical Review B* **1981**, *23*, 2004.
(38) He, J.; Wu, E.; Wang, H.; Lie, R.; Tian, Y. *Physical Review Letters* **2005**, *94*, 015504.
(39) Eremets, M. I.; Struzhkin, V. W.; Mao, H. K.; Hemley, R. J. *Science* **2001**, *293*, 272.
(40) (a) Haussermann, U.; Simak, S. I.; Ahuja, R.; Johansson, B. *Physical Review Letters* **2003**, *90*, 065701(b) Ma, Y. M.; Tse, J. S.; Klug, D. D.; Ahuja, R. *Physical Review B* **2004**, *70*, 214107.
(41) (a) Papaconstantopoulos, D. A.; Mehl, M. J. *Physical Review B* **2002**, *65*, 172510(b) Bose, S. K.; Kato, T.; Jepsen, O. *Physical Review B* **2005**, *72*, 184509.
(42) (a) Gunji, S.; Kamimura, H.; Nakayama, T. *Journal of the Physical Society of Japan* **1993**, *62*, 2408(b) Gunji, S.; Kamimura, H. *22nd International Conference on the Physics of Semiconductors* **1995**(c) Gunji, S.; Kamimura, H. *Physical Review B* **1996**, *54*, 13665(d) Hayami, W. *Physical Review B* **1999**, *60*, 1523(e) Soga, K.; Oguri, A.; Araake, S.; Terauchi, M.; Fujiwara, A.; Kimura, K. *Journal of Solid State Chemistry* **2004**, *177*, 498(f) Hayami, W.; Tanaka, T.; Otani, S. *The Journal of Physical Chemistry A* **2005**, *109*, 11975(g) Dekura, H.; Shirai, K.; Katayama-Yoshida, H. *Physica B-Condensed Matter* **2007**, *401*, 702(h) Shirai, K.; Dekura, H.; Yanase, A. *Journal of the Physical Society of Japan* **2009**, *78*, 084714(i) Dekura, H.; Shirai, K.; Yanase, A. In *16th International Symposium on Boron, Borides and Related Materials*; Tanaka, T., Ed.,

2009; Vol. 176(j) Dekura, H.; Shirai, K.; Yanase, A. *Journal of Computational and Theoretical Nanoscience* **2009**, *6*, 2629.
(43) Sadoc, J.-F.; Mosseri, R. *Geometrical Frustration*; Cambridge University Press: Cambridge, UK, 1999.
(44) Kroto, H. W.; Heath, J. R.; Obrien, S. C.; Curl, R. F.; Smalley, R. E. *Nature* **1985**, *318*, 162.
(45) (a) Belin, C.; Charbonnel, M. *Journal of Solid State Chemistry* **1986**, *64*, 57(b) Burdett, J. K.; Canadell, E. *Journal of the American Chemical Society* **1990**, *112*, 7207(c) King, R. B. *Inorganica Chimica Acta* **1991**, *181*, 217(d) Tillardcharbonnel, M.; Chouaibi, N.; Belin, C.; Lapasset, J. *Journal of Solid State Chemistry* **1992**, *100*, 220(e) Tillardcharbonnel, M.; Belin, C.; Chouaibi, N. *Zeitschrift Fur Kristallographie* **1993**, *206*, 310(f) Belin, C.; Tillard-Charbonnel, M. *Coordination Chemistry Reviews* **1998**, *178*, 529(g) Haussermann, U.; Svensson, C.; Lidin, S. *Journal of the American Chemical Society* **1998**, *120*, 3867(h) Corbett, J. D. *Angewandte Chemie-International Edition* **2000**, *39*, 670(i) Li, B.; Corbett, J. D. *Journal of the American Chemical Society* **2005**, *127*, 926.
(46) (a) Frank, F. C.; Kasper, J. S. *Acta Crystallographica* **1958**, *11*, 184(b) Frank, F. C.; Kasper, J. S. *Acta Crystallographica* **1959**, *12*, 483.
(47) Hughes, R. E.; Leonowicz, M. E.; Lemley, J. T.; Tai, L. T. *Journal of the American Chemical Society* **1977**, *99*, 5507.
(48) Machaladze, T. *Proceedings of the Academy of Sciences of Georgia, Chemical Series* **2005**, *31*, 331.
(49) Mailhiot, C.; Grant, J. B.; McMahan, A. K. *Physical Review B* **1990**, *42*, 9033.
(50) (a) Bardeen, J.; Cooper, L. N.; Schrieffer, J. R. *Physical Review* **1957**, *108*, 1175(b) Ashcroft, N. W. *Physical Review Letters* **1968**, *21*, 1748(c) Papaconstantopoulos, D. A.; Boyer, L. L.; Klein, B. M.; Williams, A. R.; Morruzzi, V. L.; Janak, J. F. *Physical Review B* **1977**, *15*, 4221(d) Richardson, C. F.; Ashcroft, N. W. *Physical Review Letters* **1997**, *78*, 118.
(51) Lu, Z. W.; Wei, S. H.; Zunger, A.; Frotapessoa, S.; Ferreira, L. G. *Physical Review B* **1991**, *44*, 512.
(52) Siberchicot, B. *Physical Review B* **2009**, *79*, 224101.
(53) (a) Johnston, H. L.; Hersh, H. N.; Kerr, E. C. *Journal of the American Chemical Society* **1951**, *73*, 1112(b) McDonald, R. A.; Stull, D. R. *Journal of Chemical & Engineering Data* **1962**, *7*, 84(c) Bogdanov, V. I.; Vekilov, Y. K.; Tsagarei.Gv; Zhgenti, I. M. *Soviet Physics Solid State,Ussr* **1971**, *12*, 2701(d) Hu, Q. L.; Noda, T.; Suzuki, H.; Numazawa, T.; Arai, O.; Hirano, T.; Nogi, N.; Tanaka, S. *Journal of Applied Physics* **2001**, *90*, 728(e) Cerqueira, A. B., MS Thesis, Dalhousie University, 2011.
(54) (a) Garbulsky, G. D.; Ceder, G. *Physical Review B* **1995**, *51*, 67(b) Ceder, G.; Garbulsky, G. D.; Tepesch, P. D. *Physical Review B* **1995**, *51*, 11257(c) Tepesch, P. D.; Garbulsky, G. D.; Ceder, G. *Physical Review Letters* **1995**, *74*, 2272(d) Wolverton, C.; Zunger, A. *Physical Review Letters* **1998**, *81*, 606.
(55) Parakhonskiy, G.; Dubrovinskaia, N.; Bykova, E.; Wirth, R.; Dubrovinsky, L. *Sci. Rep.* **2011**, *1*, 96.
(56) Ogitsu, T.; Schwegler, E. *Solid State Sciences* **2012**, 10.1016/j.solidstatesciences.2012.03.005.
(57) Fisher, M. E. *Physical Review* **1959**, *113*, 969.

(58) Ising, E. *Zeitschrift Fur Physik* **1925**, *31*, 253.
(59) (a) Wannier, G. H. *Physical Review* **1950**, *79*, 357(b) Husimi, K.; Syozi, I. *Progress of Theoretical Physics* **1950**, *5*, 177(c) Houtappel, R. M. F. *Physica* **1950**, *16*, 425(d) Wannier, G. H. *Physical Review B* **1973**, *7*, 5017.
(60) (a) Syozi, I. *Progress of Theoretical Physics* **1951**, *6*, 306(b) Kano, K.; Naya, S. *Progress of Theoretical Physics* **1953**, *10*, 158.
(61) Majni, G.; Prudenzi.M *Physica Status Solidi a-Applied Research* **1971**, *5*, K129.
(62) Golikova, O. A.; Kazanin, M. M.; Samatov, S.; Khomidov, T. *Soviet Physics Semiconductors-Ussr* **1982**, *16*, 479.
(63) (a) Slack, G. A.; Hejna, C. I.; Garbauskas, M.; Kasper, J. S. *Journal of Solid State Chemistry* **1988**, *76*, 64(b) Kobayashi, M.; Higashi, I.; Matsuda, H.; Kimura, K. *Journal of Alloys and Compounds* **1995**, *221*, 120(c) Hyodo, H.; Araake, S.; Hosoi, S.; Soga, K.; Sato, Y.; Terauchi, M.; Kimura, K. *Physical Review B* **2008**, *77*, 024515(d) Hyodo, H.; Nezu, A.; Soga, K.; Kimura, K. *Solid State Sciences* **2012**, *Accepted*.
(64) Mingos, D. M. P.; Wales, D. J. *Introduction to cluster chemistry*; Prentice Hall, Inc, 1990.
(65) Jemmis, E. D.; Balakrishnarajan, M. M.; Pancharatna, P. D. *Journal of the American Chemical Society* **2001**, *123*, 4313.
(66) (a) Ling, R. G.; Belin, C. *Zeitschrift Fur Anorganische Und Allgemeine Chemie* **1981**, *480*, 181(b) Belin, C.; Ling, R. G. *Journal of Solid State Chemistry* **1983**, *48*, 40(c) King, R. B. *Inorganic Chemistry* **1989**, *28*, 2796(d) Belin, C.; Tillardcharbonnel, M. *Progress in Solid State Chemistry* **1993**, *22*, 59(e) Belin, E.; Dankhazi, Z.; Mizutani, U.; Sadoc, A. *Journal of Non-Crystalline Solids* **1995**, *193*, 312.
(67) Imai, Y.; Mukaida, M.; Ueda, M.; Watanabe, A. *Journal of Alloys and Compounds* **2002**, *347*, 244.
(68) (a) Wade, K. *Journal of the Chemical Society D-Chemical Communications* **1971**, 792(b) Wade, K. *Inorganic & Nuclear Chemistry Letters* **1972**, *8*, 563(c) Mingos, D. M. P. *Nature-Physical Science* **1972**, *236*, 99(d) Williams, R. E. *Adv. Inorg. Chem. Radiochem.* **1976**, *18*, 67(e) Wade, K. *Adv. Inorg. Chem. Radiochem.* **1976**, *18*, 1(f) King, R. B.; Rouvray, D. H. *Journal of the American Chemical Society* **1977**, *99*, 7834(g) Stone, A. J. *Molecular Physics* **1980**, *41*, 1339(h) Mingos, D. M. P. *Journal of the Chemical Society-Chemical Communications* **1983**, 706(i) Mingos, D. M. P. *Accounts of Chemical Research* **1984**, *17*, 311(j) Wade, K. *Nature Chemistry* **2009**, *1*, 92.
(69) (a) Silvestrelli, P. L. *Physical Review B* **1999**, *59*, 9703(b) Marzari, N.; Vanderbilt, D. *Physical Review B* **1997**, *56*, 12847(c) Souza, I.; Martin, R. M.; Marzari, N.; Zhao, X. Y.; Vanderbilt, D. *Physical Review B* **2000**, *62*, 15505(d) Fornari, M.; Marzari, N.; Peressi, M.; Baldereschi, A. *Computational Materials Science* **2001**, *20*, 337(e) Souza, I.; Marzari, N.; Vanderbilt, D. *Physical Review B* **2002**, *65*, 035109(f) Calzolari, A.; Marzari, N.; Souza, I.; Nardelli, M. B. *Physical Review B* **2004**, *69*, 035108(g) Thygesen, K. S.; Hansen, L. B.; Jacobsen, K. W. *Physical Review Letters* **2005**, *94*, 026405(h) Thygesen, K. S.; Hansen, L. B.; Jacobsen, K. W. *Physical Review B* **2005**, *72*, 125119.
(70) (a) Foster, J. M.; Boys, S. F. *Reviews of Modern Physics* **1960**, *32*, 300(b) Boys, S. F. *Reviews of Modern Physics* **1960**, *32*, 296.
(71) (a) Darsavelidze, G. S.; Tsagareishvili, G. V.; Tsagareishvili, O. A.; Antadze, M. E.; Zoidze, N. A.; Dzigrashvili, T. V.; Kutelia, E. K. 9th International Symposium on Boron, Borides and Related Compounds, Duisburg, Germany, 1987; p 341(b) Tsagareishvili, G.

In *11th International Symposium on Boron, Boride and Related Compounds*; JJAP: Tsukuba, Japan, 1994; Vol. 10(c) Gabunia, D.; Tsagareishvili, O.; Darsavelidze, G.; Lezhava, D.; Antadze, M.; Gabunia, L. *Journal of Solid State Chemistry* **2004**, *177*, 600.
(72) Lonc, W. P.; Jacobsmeyer, V. P. Boron, 1965; p 215.
(73) Golikova, O. A.; Berezin, A. A.; Zaitsev, V. K.; Kazanin, M. M.; Orlov, V. M.; Stilbans, L. S.; Tkalenko, E. N. *Journal of the Less-Common Metals* **1976**, *47*, 129.
(74) Golikova, O. A.; Kazanin, M. M.; Lutsenko, E. L. *Journal of the Less-Common Metals* **1981**, *82*, 177.
(75) (a) Tsagareishvili, G. V.; Tavadze, F. N.; Kheveilidze, A. G.; Gabunia, D. L. Boron, Walsaw, Poland, 1968; p 295(b) Petrov, A. V.; Germaidz.Ms; Golikova, O. A.; Kiskachi, A. Y.; Matveev, V. N. *Soviet Physics Solid State,Ussr* **1969**, *11*, 741(c) Fuhs, W. *Physica Status Solidi* **1970**, *41*, K17(d) Siems, C. D. *Journal of the Less-Common Metals* **1979**, *67*, 155(e) Tsagareishvili, G. V.; Nakashidze, T. G.; Jobava, J. S.; Lomidze, G. P.; Khulelidze, D. E.; Tsagareishvili, D. S.; Tsagareishvili, O. A. *Journal of the Less-Common Metals* **1986**, *117*, 159(f) Darsavelidze, G. S.; Tsagareishvili, O. A.; Eterashvili, T. V.; Metreveli, V. S.; Tavadze, G. F.; Khomeriki, D. I. *Journal of the Less-Common Metals* **1986**, *117*, 189.
(76) Werheit, H.; Kummer, F. In *16th International Symposium on Boron, Borides and Related Materials*; Tanaka, T., Ed., 2009; Vol. 176.
(77) Hoffmann, S.; Werheit, H. *Solid State Sciences* **2012**, doi:10.1016/j.solidstatesciences.2012.01.025.
(78) (a) Tsagareishvili, O. A.; Chkhartishvili, L. S.; Gabunia, D. L. *Semiconductors* **2009**, *43*, 14(b) Tsagareishvili, O.; Gabunia, D.; Chkhartishvili, L. In *16th International Symposium on Boron, Borides and Related Materials*; Tanaka, T., Ed., 2009; Vol. 176.
(79) Zhang, D. M.; Gao, C. X.; Ma, Y. Z.; He, C. Y.; Huang, X. W.; Hao, A. M.; Yu, C. L.; Li, Y. C.; Liu, J.; Peng, G.; Li, D. M.; Liu, H. W.; Zou, G. *Journal of Physics-Condensed Matter* **2007**, *19*, 425216.
(80) Gabunia, D.; Tsagareishvili, O.; Lezhava, D.; Gabunia, L.; Antadze, M.; Darsavelidze, G.; Tanaka, T. *Journal of Solid State Chemistry* **2006**, *179*, 2944.
(81) Werheit, H.; Filipov, V.; Kuhlmann, U.; Schwarz, U.; Armbrüster, M.; Antadze, M. *Journal of Physics: Condensed Matter* **2012**, *24*, 175401.
(82) Linder, B. In *Thermodynamics and Introductiory Statistical Mechanics*; John Wiley & Sons: New Jersey, USA, 2004.
(83) Lewis, G. N.; Randall, M. *Themodynamics and the free energy of chemical substances*; McGRAW-HILL BOOK COMPANY, Inc.: New York and London, 1923.
(84) Schwabl, F. In *Statistical Mechanics*; Second Edition ed.; Springer: Berlin, Germany, 2006.
(85) Landsberg, P. T. *American Journal of Physics* **1997**, *65*, 269.
(86) Gokcen, N. A.; Reddy, R. G. In *Thermodynamics*; Second Edition ed.; Plenum Publishing Corporation: New York, USA, 1996.
(87) Dugdale, J. S. In *Entropy and its physical meaning*; Tayler & Francis: Philadelphia, PA, 1998.
(88) Kaufman, M. In *Principles of thermodynamics*; Marcel Dekker, Inc: Basel, Switzerland, 2002.
(89) (a) Planck, M.; Ogg, A. In *Treatise on thermodynamics (1905)*; Kessinger Publishing: La Vergne, TN, USA, 1917(b) Fermi, E. In *Thermodynamics*; dover publications inc.: NY,

USA, 1937(c) Wilks, J. *The third law of thermodynamics*; Oxford University Press: Oxford, England, 1961.
(90) Kox, A. J. *Studies in History and Philosophy of Modern Physics* **2006**, *37*, 101.
(91) (a) Hermele, M.; Fisher, M. P. A.; Balents, L. *Physical Review B* **2004**, *69*, 064404(b) Balents, L. *Nature* **2010**, *464*, 199.
(92) Long, E. A.; Kemp, J. D. *Journal of the American Chemical Society* **1936**, *58*, 1829.
(93) Tajima, Y.; Matsuo, T.; Suga, H. *Nature* **1982**, *299*, 810.
(94) Singer, S. J.; Kuo, J. L.; Hirsch, T. K.; Knight, C.; Ojamae, L.; Klein, M. L. *Physical Review Letters* **2005**, *94*, 135701.
(95) (a) Howe, R.; Whitworth, R. W. *Journal of Chemical Physics* **1989**, *90*, 4450(b) Fukazawa, H.; Ikeda, S.; Mae, S. *Chemical Physics Letters* **1998**, *282*, 215.
(96) Shalamberidze, S. O.; Kalandadze, G. I.; Khulelidze, D. E.; Tsurtsumia, B. D. *Journal of Solid State Chemistry* **2000**, *154*, 199.
(97) Will, G.; Kiefer, B. *Zeitschrift Fur Anorganische Und Allgemeine Chemie* **2001**, *627*, 2100.
(98) (a) Ceperley, D. M.; Alder, B. J. *Physical Review Letters* **1980**, *45*, 566(b) Perdew, J. P.; Zunger, A. *Physical Review B* **1981**, *23*, 5048(c) Perdew, J. P.; Burke, K.; Wang, Y. *Physical Review B* **1996**, *54*, 16533(d) Perdew, J. P.; Burke, K.; Ernzerhof, M. *Physical Review Letters* **1996**, *77*, 3865.
(99) Williamson, A. J.; Hood, R. Q.; Grossman, J. C. *Physical Review Letters* **2001**, *87*, 246406.
(100) (a) Karki, B. B.; Wentzcovitch, R. M.; de Gironcoli, S.; Baroni, S. *Physical Review B* **2000**, *61*, 8793(b) Baroni, S.; de Gironcoli, S.; Dal Corso, A.; Giannozzi, P. *Reviews of Modern Physics* **2001**, *73*, 515(c) Baroni, S.; Giannozzi, P.; Isaev, E. *Reviews in Mineralogy and Geochemistry* **2010**, *71*, 39.
(101) (a) Miller, J. *Physics Today* **2007**, *60*, 20(b) Lau, K. C.; Pandey, R. *Journal of Physical Chemistry C* **2007**, *111*, 2906(c) Tang, H.; Ismail-Beigi, S. *Physical Review Letters* **2007**, *99*, 115501(d) Li, S. F.; Gao, L.; Gong, X. G.; Guo, Z. X. *The Journal of Physical Chemistry C* **2008**, *112*, 13200(e) Lau, K. C.; Pandey, R. *The Journal of Physical Chemistry B* **2008**, *112*, 10217(f) Lau, K. C.; Orlando, R.; Pandey, R. *Journal of Physics: Condensed Matter* **2008**, *20*, 125202(g) Gonzalez Szwacki, N. *Nanoscale Research Letters* **2008**, *3*, 49(h) Ding, Y.; Yang, X.; Ni, J. *Applied Physics Letters* **2008**, *93*, 043107(i) Chernozatonskii, L.; Sorokin, P.; Yakobson, B. *JETP Letters* **2008**, *87*, 489(j) Yang, X.; Ding, Y.; Ni, J. *Physical Review B* **2008**, *77*, 041402(k) Tian, F.-Y.; Wang, Y.-X. *The Journal of Chemical Physics* **2008**, *129*, 024903(l) Singh, A. K.; Sadrzadeh, A.; Yakobson, B. I. *Nano Letters* **2008**, *8*, 1314(m) Zope, R. R.; Baruah, T.; Lau, K. C.; Liu, A. Y.; Pederson, M. R.; Dunlap, B. I. *Physical Review B* **2009**, *79*, 161403(n) Wei, G.; Yi-Bin, H.; Yu-Yang, Z.; Shi-Xuan, D.; Hong-Jun, G. *Chinese Physics B* **2009**, *18*, 2502(o) Wang, J.; Liu, Y.; Li, Y.-C. *ChemPhysChem* **2009**, *10*, 3119(p) Tang, H.; Ismail-Beigi, S. *Physical Review B* **2009**, *80*, 134113(q) Li, M.; Li, Y.; Zhou, Z.; Shen, P.; Chen, Z. *Nano Letters* **2009**, *9*, 1944(r) Li, G. Q. *Applied Physics Letters* **2009**, *94*, 193116(s) Lee, R. K. F.; Cox, B. J.; Hill, J. M. *Journal of Physics A: Mathematical and Theoretical* **2009**, *42*, 065204(t) Lee, R. K. F.; Cox, B. J.; Hill, J. M. *The Journal of Physical Chemistry C* **2009**, *113*, 19794(u) Lau, K. C.; Orlando, R.; Pandey, R. *Journal of Physics: Condensed Matter* **2009**, *21*, 045304(v) Lau, K. C.; Yap, Y. K.; Pandey, R. *B-C-N Nanotubes and Related Nanostructures* **2009**, 271(w) Jash, P.; Trenary, M. *Journal of*

Physics: Conference Series **2009**, *176*, 012011(x) Iyyamperumal, E.; Fang, F.; Posadas, A.-B.; Ahn, C.; Klie, R. F.; Zhao, Y.; Haller, G. L.; Pfefferle, L. D. *The Journal of Physical Chemistry C* **2009**, *113*, 17661(y) Hayami, W.; Otani, S. *Journal of Physics: Conference Series* **2009**, *176*, 012017(z) Botti, S.; Castro, A.; Lathiotakis, N. N.; Andrade, X.; Marques, A. L. *Physical Chemistry Chemical Physics* **2009**, *11*, 4523(aa) Özdoğan, C.; Mukhopadhyay, S.; Hayami, W.; Güvenç, Z. B.; Pandey, R.; Boustani, I. *The Journal of Physical Chemistry C* **2010**, *114*, 4362(ab) Chkhartishvili, L. *Nano Studies* **2011**, *3*, 227(ac) Penev, E. S.; Bhowmick, S.; Sadrzadeh, A.; Yakobson, B. I. *Nano Letters* **2012**, *12*, 2441.